LUND UNIVERSITY

Electrophysiological evaluation and morphology of inherited and acquired retinal diseases

Meinert, Monika

2025

Document Version:
Publisher's PDF, also known as Version of record

[Link to publication](#)

Citation for published version (APA):
Meinert, M. (2025). *Electrophysiological evaluation and morphology of inherited and acquired retinal diseases*. [Doctoral Thesis (compilation), Department of Clinical Sciences, Lund]. Lund University, Faculty of Medicine.

Total number of authors:
1

Electrophysiological evaluation and morphology of inherited and acquired retinal diseases

MONIKA MEINERT
OPHTHALMOLOGY | FACULTY OF MEDICINE | LUND UNIVERSITY
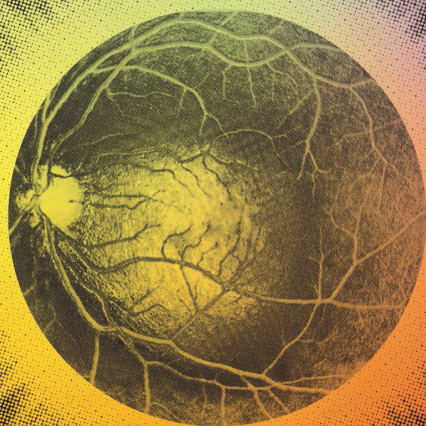
MONIKA MEINERT is a medical doctor affiliated with the Department of Ophthalmology at Skåne University hospital. Her research area is within retinal diseases. This thesis explores the electrophysiological field of retinal diseases and a novel method of structure assessment in retinal degenerative diseases.

FACULTY OF
MEDICINE

Electrophysiological evaluation and morphology of inherited and acquired retinal diseases

Electrophysiological evaluation and morphology of inherited and acquired retinal diseases

Monika Meinert, MD

LUND
UNIVERSITY

Organisation:	**Document name:**
LUND UNIVERSITY	DOCTORAL DISSERTATION
Faculty of Medicine	
Department of Clinical Sciences Lund,	**Date of issue:** 2025-09-19
Ophthalmology, Lund, Sweden	
Author: Monika Meinert	**Sponsoring organisation**

Title and subtitle: Electrophysiological evaluation and morphology of inherited and acquired retinal diseases

Abstract

Retinal degenerative diseases are characterised by progressive photoreceptor degeneration, leading to visual impairment in people worldwide. Retinitis pigmentosa (RP) is the most common inherited form, involving genes essential for photoreceptor function. Although disease progression and rate of photoreceptor death vary, RP patients often retain central vision due to preserved photoreceptor function in the macula, making this a critical region to study. Previously, detailed assessment of macular structural changes, as macular curvature, was limited. Understanding the retinal structure and functional changes is important, especially in the light of emerging gene therapies. Retinal degenerations can also provide diagnostic insight into systemic diseases, e.g. Danon disease - a rare, life-threatening condition, presenting with cardiomyopathy, characteristic retinal degeneration and electroretinography (ERG) abnormalities that can precede cardiac disease. Recognising these features can enable earlier diagnosis. Central retinal vein occlusion (CRVO), an acquired retinal disorder, is a common cause of severe vision loss in individuals over 55. Upregulation of vascular endothelial growth factor (VEGF) in CRVO causes macular oedema and vision impairment. While anti-VEGF therapy can improve vision by reducing macular oedema, only a handful of studies describe its long-term effect on photoreceptor cell function with varying results.

This thesis aims to enhance the understanding of the relationship between retinal structure, as measured by optical coherence tomography, and function, using ERG, in acquired and inherited retinal degenerative diseases.

In papers I and II, we found a high prevalence of steep macular curvature in RP eyes compared to controls. The curvature was steepest in RP eyes with preserved ellipsoid zone (EZ) width of approximately 2200 μm. Longitudinal data over a mean of 3,4 years showed progressive vertical steepening in RP eyes with preserved EZ width around 2200 μm. In paper III, we describe the ophthalmological features of Danon disease, which include a progressive retinopathy with ERG abnormalities. Additionally, a novel mosaic variant was identified, expanding the phenotypic field of the disease. In paper IV, retinal function remained reduced four years after CRVO diagnosis in both anti-VEGF treated and untreated CRVO eyes. This suggests that the disease itself has impact on retinal function and that anti-VEGF therapy does not seem to harm the photoreceptor cell function.

In conclusion, evaluation of structural and functional changes in retinal disease is crucial for understanding disease progression and for the development of future therapies, including gene therapy.

Key words: Full-field electroretinography, optical coherence tomography, retinitis pigmentosa, macular curvature, Danon disease, central retinal vein occlusion

Signature   Date 2025-08-06

Electrophysiological evaluation and morphology of inherited and acquired retinal diseases

Monika Meinert, MD

LUND
UNIVERSITY

To Emma and Matthias

"Imagination is more important than knowledge,
for knowledge is limited,
whereas imagination embraces the entire world"

Albert Einstein, Saturday Evening Post 1929

My thoughts on the thesis writing and the chosen quote:

"Imagination is a form of creative process that flourishes when intelligence is given the freedom to explore ideas with a playful and open-minded approach. And what is the thesis if not a creative process of one's scientific work?"

Table of Contents

Abstract

Retinal degenerative diseases are characterised by progressive photoreceptor degeneration, leading to visual impairment in people worldwide. Retinitis pigmentosa (RP) is the most common inherited form, involving genes essential for photoreceptor function. Although disease progression and rate of photoreceptor death vary, RP patients often retain central vision due to preserved photoreceptor function in the macula, making this a critical region to study. Previously, detailed assessment of macular structural changes, as macular curvature, was limited. Understanding the retinal structure and functional changes is important, especially in the light of emerging gene therapies. Retinal degenerations can also provide diagnostic insight into systemic diseases, e.g. Danon disease - a rare, life-threatening condition, presenting with cardiomyopathy, characteristic retinal degeneration and electroretinography (ERG) abnormalities that can precede cardiac disease. Recognising these features can enable earlier diagnosis. Central retinal vein occlusion (CRVO), an acquired retinal disorder, is a common cause of severe vision loss in individuals over 55. Upregulation of vascular endothelial growth factor (VEGF) in CRVO causes macular oedema and vision impairment. While anti-VEGF therapy can improve vision by reducing macular oedema, only a handful of studies describe its long-term effect on photoreceptor cell function with varying results.

This thesis aims to enhance the understanding of the relationship between retinal structure, as measured by optical coherence tomography, and function, using ERG, in acquired and inherited retinal degenerative diseases.

In papers I and II, we found a high prevalence of steep macular curvature in RP eyes compared to controls. The curvature was steepest in RP eyes with preserved ellipsoid zone (EZ) width of approximately 2200 μm. Longitudinal data over a mean of 3,4 years showed progressive vertical steepening in RP eyes with preserved EZ width around 2200 μm. In paper III, we describe the ophthalmological features of Danon disease, which include a progressive retinopathy with ERG abnormalities. Additionally, a novel mosaic variant was identified, expanding the phenotypic field of the disease. In paper IV, retinal function remained reduced four years after CRVO diagnosis in both anti-VEGF treated and untreated CRVO eyes. This suggests that the disease itself has impact on retinal function and that anti-VEGF therapy does not seem to harm the photoreceptor cell function.

In conclusion, evaluation of structural and functional changes in retinal disease is crucial for understanding disease progression and for the development of future therapies, including gene therapy.

Populärvetenskaplig sammanfattning

Synen, i alla dess aspekter, kan betraktas som det viktigaste av människans sinnen. Den innebär en komplex perceptionsprocess som innefattar förmågan att uppfatta färger, kontraster, seendet i både ljus och mörker, djupseende, rörelseuppfattning samt central syn som används vid läsning och perifer syn som används vid orientering.

Elektrofysiologi studerar den elektriska aktiviteten i celler, vävnader och organ, samt hur dessa genererar och överför elektriska signaler, och avspeglar därmed funktionen. Till exempel mäts hjärtats elektriska aktivitet med elektrokardiografi. För att mäta ögats elektriska aktivitet utförs fullfälts-elektroretinografi (ffERG). Undersökningen mäter näthinnefunktionen och därmed syncellernas (fotoreceptorernas) aktivitet. Näthinnan med sina fotoreceptorer och interneuroner (kopplingsnervceller) består av nervvävnad, och trots sin perifera placering, utgör den en del av det centrala nervsystemet. Näthinnan är anatomiskt uppbyggd av tio lager inklusive fotoreceptorlagret. Fotoreceptorerna delas vidare in i stavar och tappar som har olika synpigment och reagerar på olika våglängder av ljus. Stavarna är mest ljuskänsliga och ansvarar för mörkerseende, medan tapparna möjliggör dags- och färgseende. En annan anatomiskt viktig struktur i ögat är makula (gula fläcken), som mäter cirka 5,5 mm och är belägen i centrum av näthinnan i ögats bakre del. Detta område ansvarar för detaljseende samt färguppfattning, vilket behövs för att kunna läsa och känna igen ansikten. Makula utgör endast cirka 4% av näthinnans yta, men är den del av näthinnan som har högst koncentration av tappar och ger därmed också den högsta upplösningen av bilden som vi ser.

Näthinnedegenerativa sjukdomar är en grupp ögonsjukdomar, som kännetecknas av att fotoreceptorerna skadas och förlorar sin funktion, vilket orsakar synnedsättning hos människor i alla åldrar världen över. Retinitis pigmentosa (RP) är en av de vanligaste ärftliga näthinnedegenerativa sjukdomarna. Den kliniska bilden varierar mycket mellan individer och de olika genetiska varianterna, både beträffande symptombild, debut och hur snabbt sjukdomen utvecklas. De klassiska symptomen vid RP är gravt nedsatt och/eller avsaknad av mörkerseende (nattblindhet), krympande sidoseende, som i takt med att sjukdomen fortskrider resulterar i tunnelseende eller blindhet till följd av kontinuerlig fotoreceptordöd. Gemensamt för RP-patienter är att de många sjukdomsorsakande generna ofta är involverade i fotoreceptorernas uppbyggnad, ämnesomsättning eller funktion. Sjukdomsförloppet, och därmed graden av synnedsättning och fotoreceptordöd, progredierar från barndom till vuxen ålder, men ofta kvarstår ett område med fungerande fotoreceptorer i makula under lång tid, med bevarad syn i detta område. Därav är makulaområdet av stort intresse. Under de senaste åren har flera forskargrupper rapporterat om förändringar i ögats bakre del, inklusive makula, med sjuklig utbuktning av ögats vägg (så kallat stafylom), i kombination med näthinnedegeneration, särskilt hos patienter med tidiga former av RP, en

sjukdomsform som brukar kallas Lebers kongenitala amauros. Däremot finns det begränsat med rapporter om stafylom hos vuxna patienter med näthinnedegenerativa sjukdomar. Tidigare fanns inga metoder som detaljerat kunde bedöma stafylom-liknande förändringar i ögat, även om tekniker såsom ultraljud, datortomografi eller magnetisk resonanstomografi utfördes tillsammans med ögonbottenfotografering eftersom dessa metoder är otillräckliga för att noggrant studera ögats mest detaljerade strukturer, t.ex. näthinnan och fotoreceptorerna. Med utvecklingen av avbildningstekniken optisk koherenstomografi (OCT) under slutet av 1990-talet har högupplösta bilder av näthinnans cellager möjliggjorts. I kombination med framsteg inom molekylärbiologi och genetik (t.ex. next-generation sequencing, NGS), har betydande framsteg gjorts i diagnostiken och förståelsen av förvärvade och ärftliga näthinnesjukdomar.

I artikel I och II undersökte vi strukturella förändringar i ögats bakre del, specifikt i makularegionen hos RP patienter med en ny teknik som är baserad på OCT. Förändringarna beskrevs med hjälp av ett mått som kallas Mean Macula Curvature Index (MMCI). Med tekniken fann vi en hög förekomst av stafylomförändringar i makula hos RP patienter jämfört med friska individer. Makulakurvaturen var mest uttalad i RP-ögon med bevarad fotoreceptorstruktur, d.v.s. med en bevarad ellipsoidzon med cirka 2200 µm längd eller mer. Vi tittade även på hur makulakurvaturen ändrade sig över tid hos RP patienter med bevarad fotoreceptorstruktur och fann att i genomsnitt under 3,4 år skedde en progressiv ökning av makulakurvaturens vertikala axel (mätt med den nya OCT-tekniken). Detta sågs primärt hos RP patienter med bevarad fotoreceptorfunktion, d.v.s. där den ellipsoida zonen endast var lätt påverkad, och mätte 2000 µm eller mer.

Förekomsten av näthinnedegeneration kan också vara det första tecknet på allvarlig systemisk sjukdom, till exempel Danons sjukdom, ett sällsynt, livshotande tillstånd vilket yttrar sig i svår hjärtmuskelsjukdom (kardiomyopati) hos unga individer. Sjukdomen ger karakteristiska näthinneförändringar och avvikelser i ERG, som kan föregå hjärtsjukdomen. Att känna igen de typiska näthinneförändringarna kan möjliggöra tidigare diagnos och en möjlighet till rätt behandling i rätt tid av hjärtsjukdomen. I artikel III beskriver vi de oftalmologiska förändringarna i näthinnan som kännetecknar Danons sjukdom, med en fortskridande näthinnedegeneration och avvikelser i ERG. Dessutom beskrivs en ny genetisk mosaikvariant i *LAMP2*-genen, vilket ökar förståelsen av det kliniska och genetiska spektrumet av sjukdomen.

Central retinal venocklusion (CRVO) är en vanlig orsak till synnedsättning hos personer över 55 år och är ofta associerad med högt blodtryck. Det naturliga förloppet vid CRVO är vanligtvis förknippat med en dålig synprognos. Vid CRVO ses en förhöjd nivå av vaskulär endotelial tillväxtfaktor (VEGF) i näthinnan, vilket har visat sig vara en huvudsaklig bidragande orsak till svullnad (ödem) i makula och därmed nedsatt syn. I början av 2000-talet, i samband med utvecklingen av terapeutiska substanser riktade mot makulaödem, så kallade anti-VEGF preparat, blev det möjligt

att delvis återställa synfunktionen. Behandlingen kräver dock upprepade injektionsbehandlingar i ögonen över tid och det finns få rapporter om hur dessa läkemedel påverkar fotoreceptorernas funktion på lång sikt. I artikel IV studerade vi de långsiktiga effekterna av behandlingen med anti-VEGF och dexametason på näthinnans struktur och funktion hos patienter med CRVO, och jämförde resultaten med obehandlade CRVO-ögon i syfte att utvärdera långtidseffekterna på fotoreceptorernas funktion. Resultaten i artikel IV visade att näthinnefunktionen förblev fortsatt nedsatt fyra år efter CRVO diagnosen, både i ögon som behandlats med anti-VEGF och i obehandlade ögon. Detta tyder troligen på att sjukdomen i sig påverkar näthinnefunktionen, och att anti-VEGF-behandling inte verkar skada fotoreceptorcellernas funktion i CRVO-ögon ytterligare på lång sikt.

Sammanfattningsvis syftar denna avhandling till att fördjupa förståelsen av sambandet mellan näthinnans struktur och funktion vid såväl förvärvade som ärftliga näthinnedegenerativa sjukdomar. Bedömningen av strukturella och funktionella förändringar i ögat är av stor vikt, då den kan bidra till tidigare diagnos, ökad kunskap om sjukdomsutvecklingen och bättre övervakning av sjukdomsförloppet. Detta är även centralt för utvecklingen av framtida behandlingar, inklusive anti-VEGF-terapier och genterapi, som båda kräver livsdugliga fotoreceptorer och goda strukturella förhållanden i näthinnan för fotoreceptorernas överlevnad.

Papers included in this thesis

This thesis is based on the following four papers, which will be referred to in text as paper I-IV.

I.   Komori S, Ueno S, Ito Y, Sayo A, **Meinert M**, Kominami T, Inooka D, Kitagawa M, Nishida K, Takahashi K, Matsui S, Terasaki H. Steeper Macular Curvature in Eyes With Non-Highly Myopic Retinitis Pigmentosa. Invest Ophthalmol Vis Sci. 2019 Jul 1;60(8):3135-3141.

II.   **Meinert M**, Ueno S, Komori S, Koyanagi Y, Sayo A, Andreasson S, Kominami T, Ito Y, Terasaki H. Longitudinal Changes of Macular Curvature in Patients with Retinitis Pigmentosa. Transl Vis Sci Technol. 2020 Sep 10;9(10):11.

III.   **Meinert M**, Englund E, Hedberg-Oldfors C, Oldfors A, Kornhall B, Lundin C, Wittström E. Danon disease presenting with early onset of hypertrophic cardiomyopathy and peripheral pigmentary retinal dystrophy in a female with a de novo novel mosaic mutation in the *LAMP2* gene. Ophthalmic Genet. 2019 Jun;40(3):227-236.

IV.   **Meinert M**, Wittström E. Longterm visual outcome and retinal function with and without intravitreal treatments in eyes with central retinal vein occlusion. Eur J Ophthalmol. 2025 Jun 11:11206721251349247. Epub ahead of print. PMID: 40495605.

Abbreviations

AF	Autofluorescence
AL	Axial length
Anti-VEGF	Anti-vascular endothelial growth factor
AVV	Adenovirus associated vector
BG	Blueprint genetics
CFT	Central foveal thickness
CRA	Central retinal artery
CRVO	Central retinal vein occlusion
DNA	Deoxyribonucleic acid
ERG	Electroretinography
ETDRS	Early Treatment of Diabetic Retinopathy study
EZ	Ellipsoid zone
FAF	Fundus auto fluorescence
FFERG	Full-field Electroretinography
ICG	Indocyanine green
IRD	Inherited retinal diseases
ISCEV	International society for clinical electrophysiology of vision
LAMP-2	Lysosome associated membrane protein-2
LAMP 2 gene	Lysosome associated membrane protein gene
MMCI	Mean Macular Curvature Index
MFERG	Multifocal Electroretinography
NGS	Next-Generation Sequencing
OCT	Optical coherence tomography
OMIM	Online Mendelian Inheritance in Man
PPRD	Peripheral pigment retinal dystrophy
RP	Retinitis pigmentosa
RPE	Retinal pigment epithelium
VEGF	Vascular endothelial growth factor

Introduction

Vision, in all its aspects, could arguably be considered the most important of the human senses. It is a complex perception process that includes the ability to perceive colours, contrast, vision in both light and darkness, depth perception and motion detection, and peripheral vision. The visual process begins when light enters the eye through its anterior segment, comprising the cornea and lens, and is further transmitted to the posterior segment where it reaches the light sensitive neural retina. The retina contains photoreceptor cells that convert the light signal into an electric impulse, a process known as the phototransduction cascade (1). The impulse is then further delivered across retinal cells through the optic nerve, which carries the signal to the visual cortex in the occipital lobe of the brain where the visual perception takes places.

The principles of electrophysiology

Electrophysiology studies the electrical activity of cells, tissues and organs and how they generate and transmit electrical signals. Electrical signals are generated by ion movement (such as Na^+, Ca^{2+} and Cl^-) due to unequal distribution of ions inside and outside the cells and is transmitted via action potentials. It plays a crucial role in understanding the function of the central nervous system (CNS), including the eye, but also other organs such the heart and skeletal muscles (2).

Visual electrophysiology

To assess electrical activity in the eye, specifically the retina with its photoreceptor cells, an electroretinogram is performed. The first electroretinography (ERG) recordings were conducted on frogs by the Swedish ophthalmologist F. Holmgren in Uppsala in 1865 (3). However, the first ERG conducted on human eyes was performed by Dewar in Scotland in 1877 (4). Since its development, ERG has evolved into a standard method of diagnosing and monitoring inherited retinal diseases (IRD). The ERG records the electrical responses of retinal cells generated in response to light. The ERG response to light consists of three components: a-, b-

and c-waves. The cellular origin of the waves has been debated; however, the a-wave, the first negative response, comes from photoreceptors (5, 6). The origin of the b-wave, the second positive wave, has been more debated, but recent research suggests that the b-wave arises from bipolar cells (7, 8) and partially in association with Müller cells (9). The c-wave reflects the activity of the retinal pigment epithelium cells (RPE), but is not used in clinical practice (10). The a- and b-waves are shown in Figure 1. The amplitudes of the ERG response can be said to roughly represent the photoreceptor 'strength' and are measured in microvolts (μV). The a-wave amplitude is measured from baseline (no response) to the deepest trough and represents the 'health' of the photoreceptors in the outer retina. However, the b-wave amplitudes are measured from the a-wave trough to maximum peak response of the b-wave and represent the 'health' of the bipolar cells and Müller cells (9). The implicit time reflects the speed of transmission of the light signal and is measured in milliseconds (ms). In the a-wave, the implicit time is measured from the onset of the light stimulus to the trough; in the b-wave to the peak of the b-wave (Figure 1).
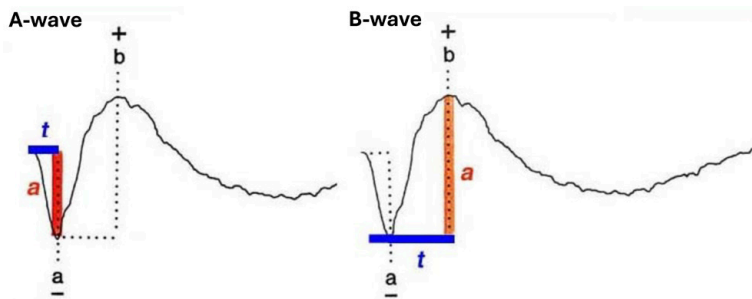
Figure 1. Amplitude and implicit time measurements of the electroretinogram waveform. The a-wave (**a**), representing photoreceptor function, presented with implicit time (t, blue line) and amplitude (a, red line). The b-wave (**b**), representing bipolar cell activity with contribution of Müller cells presented with implicit time (t, blue line) and amplitude (a, orange line) reprinted with permission by Helga Kolb is licensed under CC BY-NC (11).

Full-field ERG (ffERG) is used to assess the retinal response to light stimuli delivered by a Ganzfeld sphere. The technique uses light stimulus at varying wave lengths, light intensities and frequencies to elicit responses from rod and cone photoreceptors under both scotopic (dark-adapted) and photopic (light-adapted) conditions. In the dark-adapted retina, the ffERG generates very weak flashes of white or, in some instances, blue light to elicit isolated rod responses, a single flash of white light to elicit combined rod-cone response (representing the total retinal function), and bright single flash white light with background light and 30 Hz flicker to evaluate the isolated cone responses, as the rods cannot respond to a light stimulus above 20 Hz. The International Society for Clinical Electrophysiology of Vision

(ISCEV) has established a standardised protocol in order to synchronize ERG recordings, ensuring comparative results worldwide (12). This protocol is continuously updated, and additional testing procedures are added for better interpretation of retinal function assessed by electroretinography (13). Overall, ffERG is a non-invasive and well-established method to measure the functioning of the entire retina. FfERG recording of human retina is showed in Figure 2.
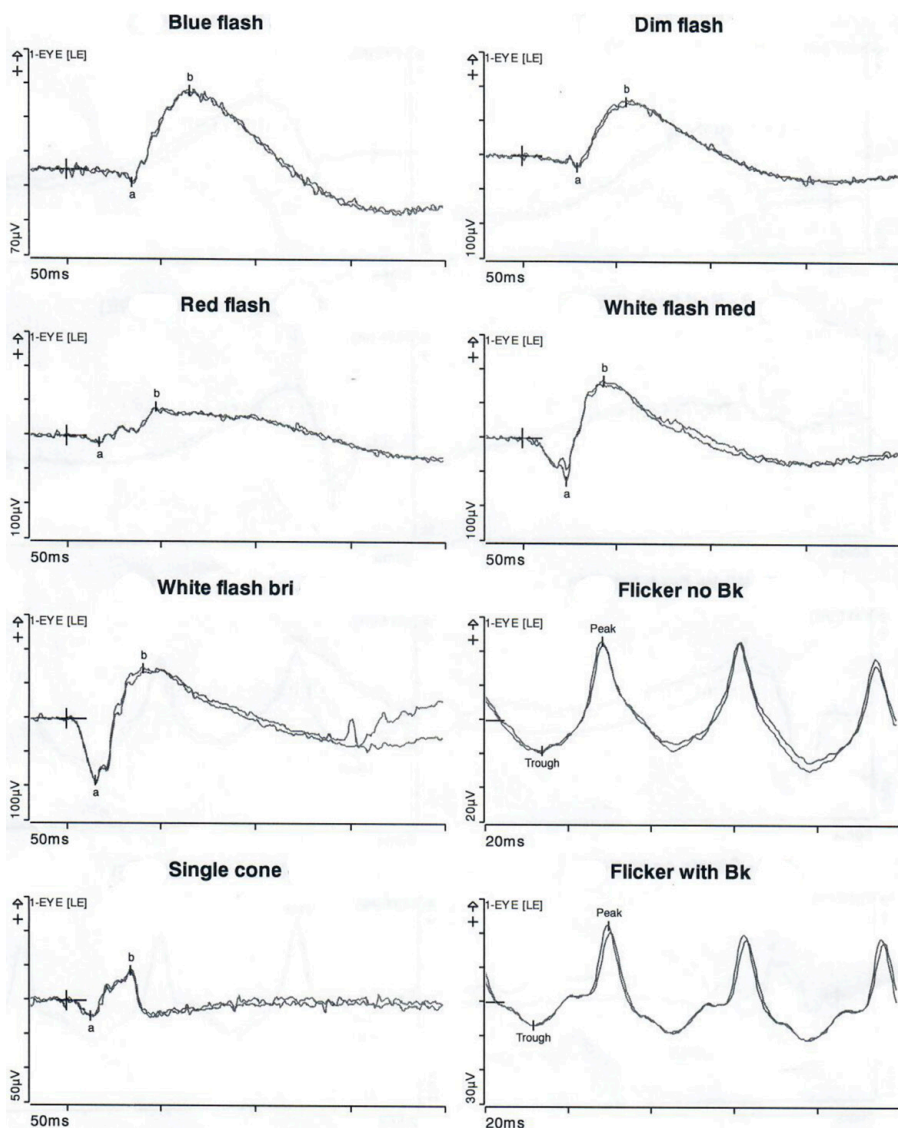
Figure 2. Full-field electroretinograms from a healthy human retina. Presenting with an a-wave (a) and b-wave (b) in response to different light stimulus using the Diagnosys system.

Multifocal ERG (mfERG)

Multifocal electroretinography (mfERG) is an advanced technique used to assess function of the central retina under light-adapted conditions, specifically focusing on macular function, especially the cone photoreceptors. The technique was developed in 1992 by E. Sutter and colleagues. The mfERG uses mathematical sequences consisting of over 100 focal responses that simultaneously stimulate multiple areas of the central retina, enabling data collection over several minutes (14). The mfERG consists of 61 or 103 hexagons that shift rapidly between black and white, i.e. on- and off- light stimulus, on a frame at a rate of 75 Hz. The white hexagon is a light stimulus with a white flash of light >100 cd/m^2 and generates a retinal response. The black hexagon, without light stimulus, generates no retinal response (15). The recorded responses of mfERG are extracted from continuous measurement and consist of three waves, first a negative wave (N1) followed by a positive wave (P2) and a negative wave (N2). The waves are measured with implicit time and amplitudes. The cellular response from mfERG is mainly contributed from cones and bipolar cells. ISCEV provides the standard protocol for mfERG, which is continuously updated (15) (Figure 3).
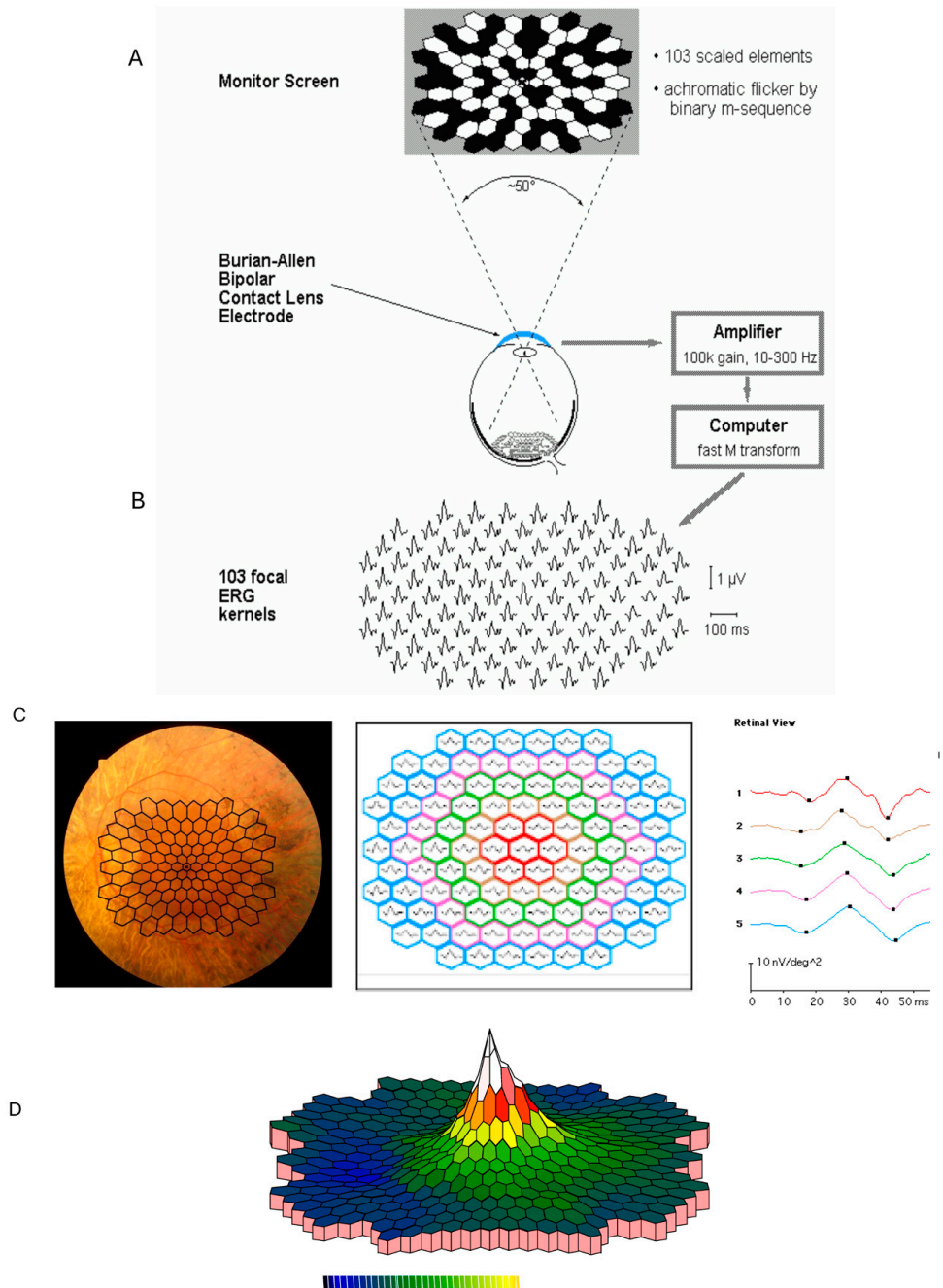
Figure 3. Multifocal electroretinography recordings in a healthy human retina. (A) The stimulating picture from the monitor screen. (B) The electrical response are shown as trace arrays for each of the 103 hexagons of the stimulus pattern. (C) The curves reflecting the summed reponses from multiple hexagons arranged as rings from the centre and outwards and (D) 3D-topography plot with the centred top correspoding to the cone function in fovea.

Human retina anatomy

Despite its peripheral location, the retina is an extension of the CNS and made of neural tissue located in the posterior part of the eye (16). Morphologically, the retina consists of several layers, including the photoreceptors, which are localised in the outer part of the retina. Photoreceptors are further divided into cones and rods, which have different visual pigments and respond to different wave lengths of light. Rods are sensitive to dim light and are responsible for our night vision (17). Rods contain the visual pigment rhodopsin and are sensitive to blue-green light with a peak sensitivity around 500 nm. Conversely, the cones are responsible for daytime- and colour vision and contain three different visual pigments, cone opsins, which are further subdivided into 3 groups depending on which wavelength of light they capture. The blue cones (short wavelength, approximately 420 nm), the green cones (middle wavelength, approximately 530 nm) and red cones (long wavelength, approximately 560 nm) (18). There are about 5 million cones in the retina, mostly concentrated in the central retina, in the macula, and with lower density throughout the peripheral retina. The rods are numerous, more than 100 million, and distributed throughout the entire retina, except for the centre of the eye, the macula (19, 20) (Figure 4).
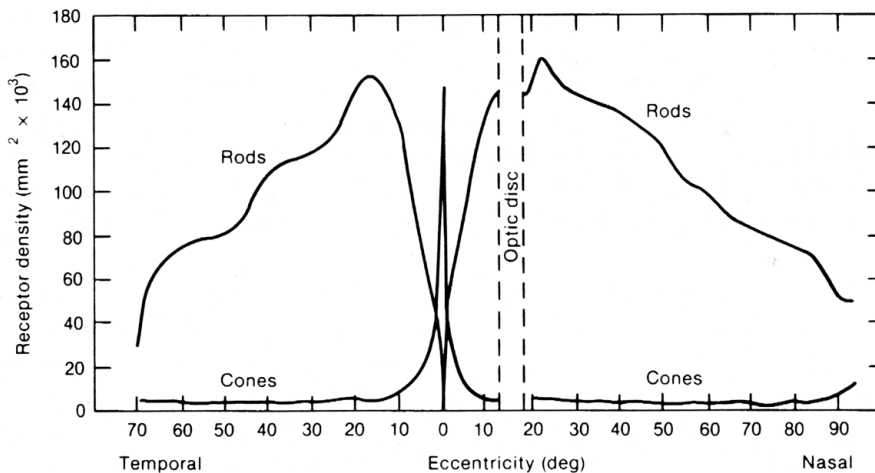
Figure 4. Distribution of rod and cones in normal human retina. From Österberg 1995.

The retinal morphology

The retina is further subdivided into ten layers seen from how the light enters the eye:

- Internal Limiting Membrane (ILM) - this structure connects the Müller cells to the vitreous body.

- Retinal Nerve Fibre Layer (RNFL) - is composed of axons of ganglion cells that form the optic nerve.

- Ganglion Cell Layer (GCL) - consisting mainly of cell bodies of ganglion cells and displaced amacrine cells.

- Inner Plexiform Layer (IPL) - occupied by synapses between bipolar cells and amacrine and ganglion cells.

- Inner Nuclear Layer (INL) - containing cell bodies of bipolar, horizontal amacrine cells.

- Outer Plexiform Layer (OPL) - occupied by synapses between rod-cone photoreceptors with bipolar and horizontal cells. Capillaries are also found in this layer.

- Outer Nuclear Layer (ONL) - consisting of the rod and cone photoreceptor cell bodies and Henle fibre layer (photoreceptor oblique axons and Müller cell processes).

- External Limiting Membrane (ELM) - occupied by junction complex between inner segments (IS) of photoreceptors and Müller cells.

- Photoreceptor layer - layer of inner segment of photoreceptor, Ellipsoid Zone (EZ) and outer segment of photoreceptors, Interdigitation Zone (IZ).

- Retinal Pigment Epithelium (RPE) - supportive cells for the retina located between photoreceptors and Bruch's membrane that perform many functions, including making up the blood-retinal barrier (21)(Figure 5).
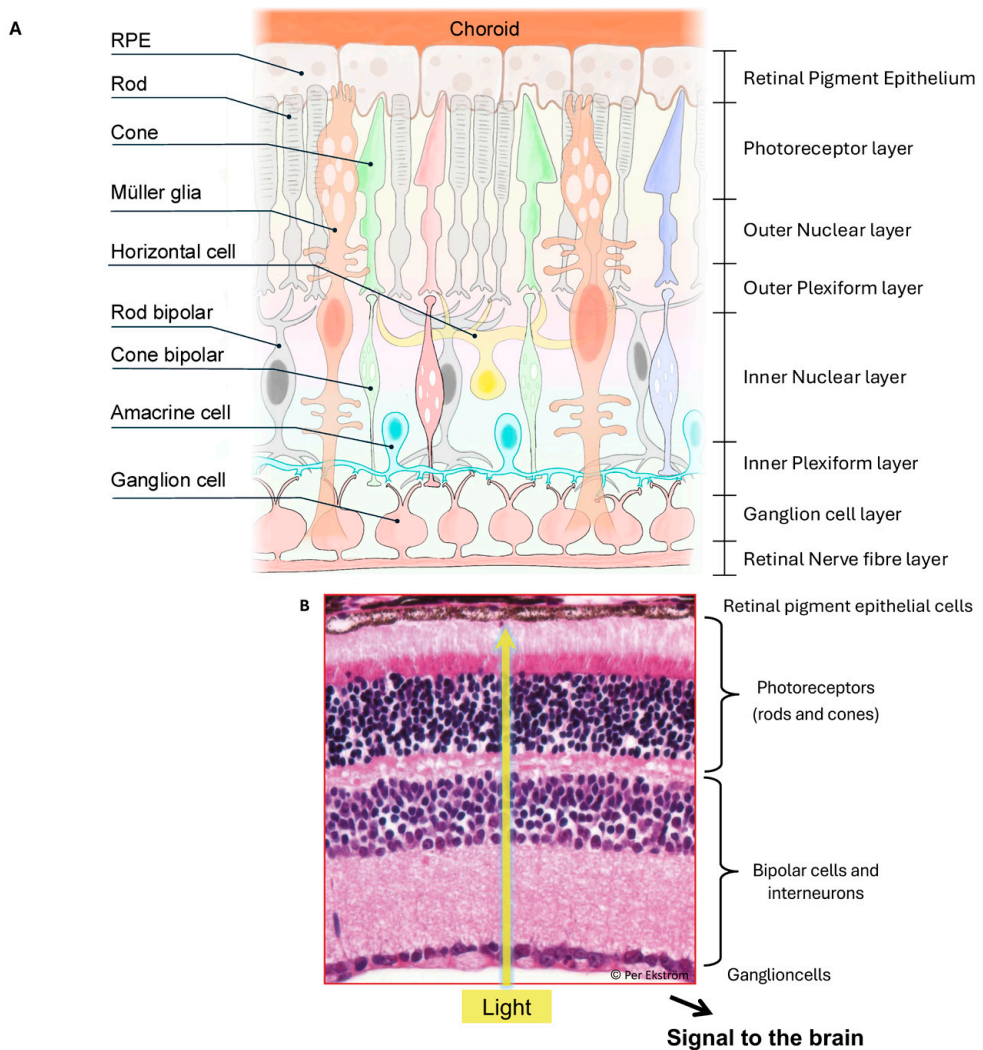
Figure 5. (A) Showing a schematic drawing of healhy human retina. (B) Showing retinal layers in light micrograph of a vertical section through healthy mouse retina. (B) With permission from Per Ekström, Lund University 2025.

The macula

The macula is an anatomical structure in the centre of the eye measuring approximately 5.5 mm in diameter and is located 4.5-5 mm temporal from the optic nerve (22). The macula is recognisable to ophthalmologists as the 'macula lutea', the yellow spot, due to its yellow reflection. This reflection is due to the pigments xanthophyll and the carotenoids zeaxanthin and lutein, which are present in cone axons and Henle´s fibre layer (23). The macula is responsible for detailed vision,

colour perception and detailed visual tasks such as reading or face recognition thus an essential part of human vision. It makes up just 4 % of the retinal surface, but has a higher concentration of cones and ganglion cells than the rest of the retina (17). In the centre of the macula is a specialised pit-shaped region, the fovea, measuring approximately 1.0-1.5 mm in diameter and 200-240 μm deep (24). This area provides the sharpest vision and contains a high density of cones, and is rod- and vessel-free, and is also referred to as the foveal avascular zone (FAZ). At the centre of the fovea lies the foveola, which measures around 0.35-0.5 μm in diameter and has a retinal thickness of 100 μm (25). This is where the visual acuity is at its highest. It contains the highest density of packed cones and is, like the fovea entirely rod- and vessel-free. The high density of cones and one-to-one relationship with bipolar cells makes it possible to mediate the very high visual resolution of the macula (26, 27) (Figure 6).
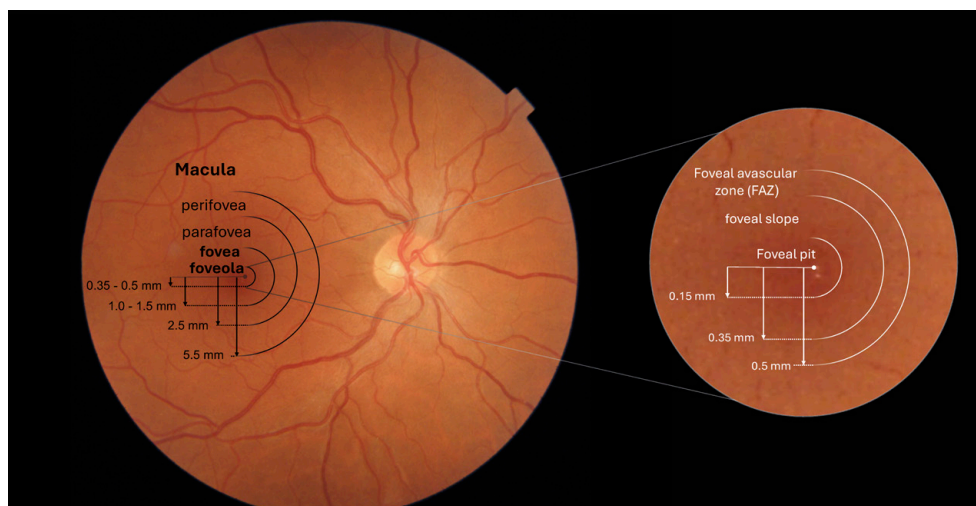
Figure 6. Map of the macular area, presenting the dimensions of the perifovea, parafovea, fovea, and foveola. The insert presents the foveal avascular zone.

Other important cells in the retina that play a key role in processing visual images are the bipolar, ganglion cells, Müller cells and RPE (28). The bipolar cells receive light signals from rod-cone photoreceptors and project their axons onto the ganglion cells, whose axons form the optic nerve and send the visual signal along the optic nerve to the brain cortex. The Müller cells provide structural and metabolic support and cover the entire thickness of the retina (29).

The RPE is a layer of epithelial cells containing melanin granules, giving it a pigmented appearance. They are situated between the photoreceptors and the choroid, and through their tight junctions they make up a part of the important barrier between

the retina and the systemic circulation (blood-retinal barrier). RPE performs several important tasks that are essential for visual functioning, such as phagocytosis of photoreceptor outer segments, transporting metabolites and ions to and from the retina and recycling vitamin A (30). The RPE also contains a second granule, lipofuscin, which is a waste product from degraded photoreceptors' outer segments. With age, lipofuscin granules are aggregated in the RPE and can subsequently compromise the function of this cell layer. A disrupted RPE can indicate a dysfunction, such as seen in macular oedema, and be a sign of an IRD (31).

Retinal blood supply

The retina is supplied by two arterial systems: the choroidal blood vessels (through short posterior ciliary arteries, branches of ophthalmic artery), which account for approximately one-third of the blood flow and are essential for the outer retina containing the photoreceptors and RPE; and the central retinal artery (CRA) (Figure 7). The CRA branches of the ophthalmic artery, which branches of the internal carotid artery, and it constitutes the remaining two-thirds of blood flow, supplying the inner retinal layers. The venous blood outflow of the retina drains via the central retinal vein (CRV), its branch retinal veins, capillary plexus and perivenular drainage. The CRV is the main vessel that drains the retina and runs alongside the CRA. It leaves the eye through the optic disc, where it drains into the superior ophthalmic vein or cavernous sinus. The capillary plexus (CP) is divided into the superficial CP, located in the NFL and GCL and the deep CP located within the INL. However, the blood drainage from the photoreceptors in the ONL is performed by choroidal circulation drained by the vortex veins (22, 32).
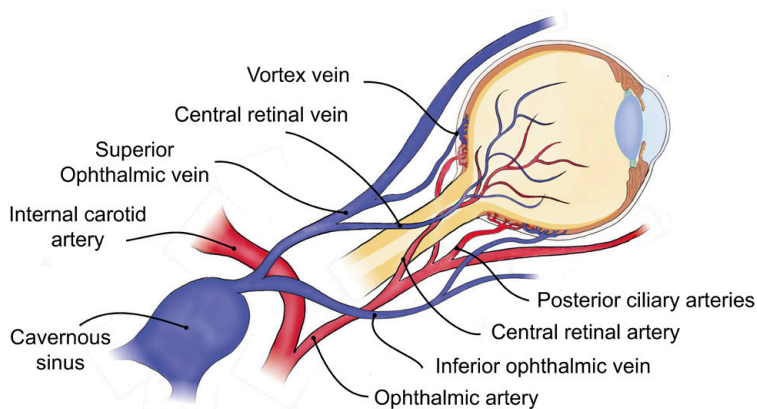
Figure 7. Blood supply of the orbit and retina.

Advances in retinal imaging

The development of retinal imaging techniques in the late 90s, such as optical coherence tomography (OCT), made it possible to provide detailed high-resolution images of the retinal structure. This non-invasive imaging technique works in a similar way to an ultrasound, but instead of sound it uses light waves to create detailed, high-resolution cross-sectional images of retinal cell layers. OCT measures the backscattered or back-reflected light, allowing us to visualise the retinal microstructure in high resolution (Figure 7). OCT can provide cross-sectional images of retinal structure and morphology in a μm resolution and in real-time. This technique has revolutionised ophthalmology care, including aiding in diagnosing diseases, understanding the retinal pathology and allowing clinicians to evaluate disease progression and assess response to treatment. Nowadays OCT is considered as standard care in ophthalmology (33).

Retinal layers identified by OCT
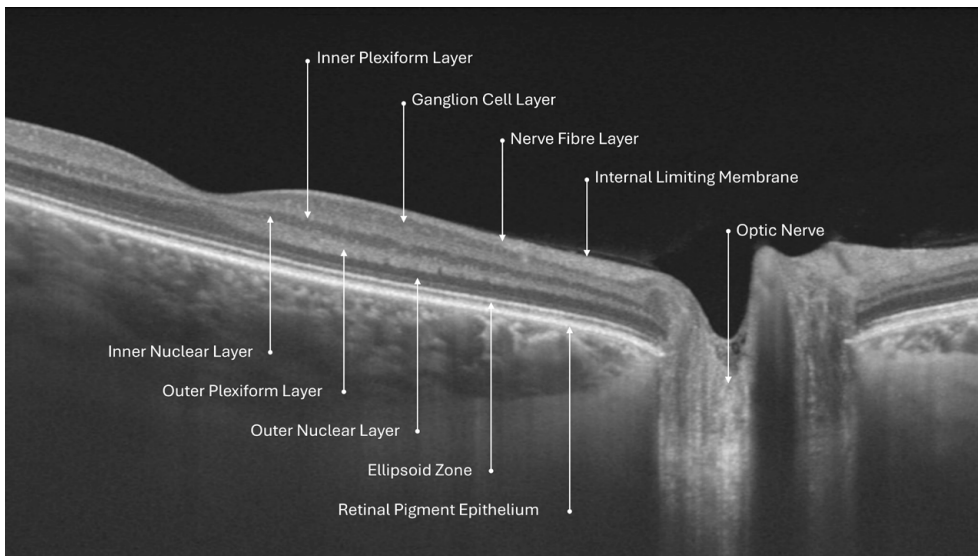
Figure 8. Retinal layers of a normal human retina imaged with optical coherence tomography.

The photoreceptor layer on OCT, Ellipsoid Zone

The Ellipsoid Zone corresponds to the inner segments of photoreceptors. It is visualised on the OCT-scans as the second hyperreflective band (34, 35) (Figure 8).

These segments are densely packed with mitochondria and reflect the health of the photoreceptors. A well-defined EZ suggests healthy photoreceptors, while disruption can indicate retinal disease. The most central ellipsoid zone corresponds to mfERG photoreceptor cell function (36) and analysis of this layer with OCT is a reliable method of evaluating the progression rate of photoreceptor degeneration in RP (37, 38).

Retinal degenerative diseases

Inherited retinal diseases

Retinal degenerative diseases are a group of ocular disorders characterised by photoreceptor dysfunction and degeneration that cause visual impairments among people worldwide. To date, we know approximately 350 genes with clinical manifestation of IRD, which are described in the Online Mendelian Inheritance in Man database (OMIM, https://omim.org), and in RetNet (https://retnet.org).

Retinitis pigmentosa is one of the major IRDs, which presents with clinical and genetic heterogeneity. Although clinically variable, the classical symptoms include difficulties with dark adaptation and/or night blindness from a young age and progressive visual field loss that often starts in midperiphery and progresses to a loss of the peripheral visual fields as the disease advances. At present, approximately 70 genetic variants have been identified that are correlated with RP, but additional genes are continuously being identified (39). The prevalence of RP is approximately 1:3500 individuals worldwide. RP can be inherited, e.g. as autosomal recessive (AR), which represents approximately 60% of cases, autosomal dominant (AD) in 30-40% of cases, and X-linked (XLRP), which represents approximately 5-15% of cases (40, 41). However, RP can be part of new pathogenic genetic variants, such as non-Mendelian inheritance patterns (digenic or mitochondrial inheritance), although these variants seem to represent a smaller portion of cases (42, 43). The many different disease-causing genes are typically involved in the photoreceptor function, causing a rod-cone degeneration. The rate of photoreceptor death, visual impairment and disease progression varies from young age to adulthood; however, these patients often have a remaining zone with residual photoreceptors in the macular region for a long period of time (44). These patients usually also have remaining vision related to this area, making this a region of major interest. In recent years, several authors have reported about changes in the posterior segment, including staphyloma and coloboma in combination with widespread retinal degeneration, especially found in early forms of RP such as Leber's congenital amaurosis (LCA) with known genotypes: *NMNAT1, IDH3A, DHX38, RDH12* and *CEP290* (45-48). However, there are limited reports of adult patients with retinal

degenerative diseases and staphyloma formation in the posterior pole (49, 50). In 2018, no accurate methods capable of evaluating staphyloma-like alterations with precision were available, since prior techniques, including ultrasound, computed tomography and magnetic resonance imaging together with fundus photography (51), were all inadequate for an in-depth examination of the ocular structures, specifically for the retina and photoreceptors. With the development of retinal imaging techniques in the late 90s, such as OCT, which generate high-resolution images of the cellular layers of the retina, it became possible to assess structural changes at cellular levels.

Assessing structural changes contributes to further understanding of the disease development and better monitoring of disease progression. Evaluating structural changes of the posterior pole is also of importance, since gene therapy is an upcoming treatment in RP and the benefit of gene therapy lies in preserving still viable photoreceptors that also need proper structural conditions for their survival (Figure 9).
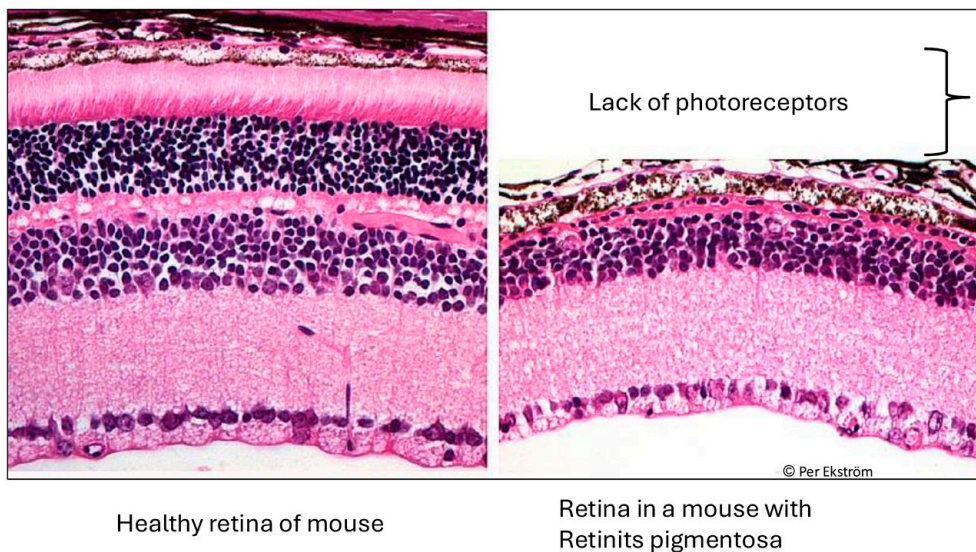
Figure 9. Light microscopy images of healthy mouse retina and pathologic retina in a mouse with retinitis pigmentosa. With permission from Per Ekström 2025, Lund University.

Danon disease is a rare disease that clinically presents with progressive cardiomyopathy, neuromuscular disorders and various levels of intellectual disability (52) and retinal dystrophy (53, 54). The disease was genetically identified in 2000 by Nishino et al. (55) and is associated with lysosomal defects due to a pathogen variant in the lysosome-associated membrane protein2 (*LAMP2*) gene (55, 56). In Danon disease the genetic variant leads to an absence of protein expression

of LAMP2 which leads to an accumulation of autophagic material and glycogen in the cardiac muscle's and skeletal muscle's cells (55). Ophthalmological features of Danon disease with a *LAMP2* variant include characteristic peripheral pigmentary retinal dystrophy (PPRD), with varying loss of RPE and variability of cone-rod dystrophy as well as ERG abnormalities (57) that can be present before the onset of severe cardiac disease. Ophthalmologic findings are thoroughly described in just a few studies (58, 59). Danon disease is inherited in an X-linked dominant pattern, which means males are more severely affected than females. However, genetic identification has been particularly difficult in female patients and in mosaic carriers of the *LAMP2* genetic variant (58-60). Early identification of the disease is crucial, as it can progress rapidly to cardiac dysfunction and sudden death in young patients.

Acquired retinal diseases

Central retinal vein occlusion (CRVO) is a common cause of severe vision loss in individuals over 55 years of age and the second most common vascular disease after diabetic retinopathy (61). The most important risk factors associated with CRVO are systemic hypertension, diabetes mellitus, hyperlipidaemia and ocular risk factors including ocular hypertension and glaucoma (62, 63).

CRVO is further divided into two subtypes, non-ischemic and ischemic, and has poor visual outcome when following its natural course, especially the ischemic subtype of CRVO (64). An upregulation of vascular endothelial growth factor (VEGF) is present in CRVO eyes, especially in the ischemic type, and has been found to be a major contributor to macular oedema and consequently vision impairment (65, 66). With the development of anti-VEGF agents, treatment of macular oedema is possible, and the visual outcome has significantly improved in CRVO eyes, as many large prospective studies have shown, including CRUISE, GALILEO and COPERNICUS (67-69). However, in a majority of the CRVO patients, the anti-VEGF treatments need to be given continuously to prevent recurrence of macular oedema and consequently vision impairment (69, 70). Furthermore, only a few studies have examined the long-term effect of anti-VEGF agents on photoreceptor cell function in CRVO eyes using ERG, with varying results (71-73). The degree of retinal ischemia in CRVO has an impact on retinal function and is reported to correlate significantly to the implicit time of the 30Hz flicker ERG (74, 75). ERG is proposed to be a more accurate method to evaluate retinal ischemia than 'gold standard' methods such as perimetry or fluorescein angiography (FA) (76).
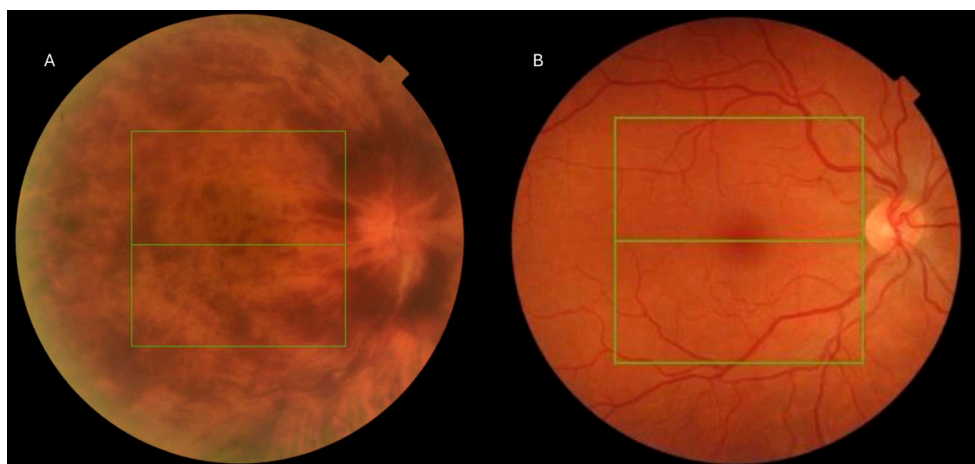
Figure 10. (A) Fundus photo of a patient in study IV with central retinal vein occlusion with multiple retinal bleeds and macular and optic nerve head oedema. (B) Fundus photo of healthy human retina.

Anti-vascular endothelial growth factor therapy in ophthalmology

The anti-VEGF therapy emerged in ophthalmology in the early 2000s after the significant role of VEGF in pathological neovascularisation in the eye became understood (77), particularly in choroidal neovascularisation of age-related macular degeneration (wet-AMD) (78) and in CRVO (65). Ranibizumab (Lucentis), a monoclonal antibody fragment specially engineered to bind to VEGF-A, was approved by the U.S. Food and Drug Administration (FDA) in 2006 as the initial intravitreal treatment for wet-AMD. This remarkable drug not only halted the decline of visual acuity (VA), but also improved VA in significant percentages of patients with wet-AMD during pivotal phase III of clinical trials (79). Five years later, another anti-VEGF drug, Aflibercept (Eylea), was FDA approved. Aflibercept is a fusion protein of VEGF receptors and has the affinity to bind VEGF-A, VEGF-B and placental growth factor, and its area of use has expanded to treat many retinal diseases with macular oedema, including CRVO (68-70). Another intravitreal therapy is the corticosteroid-based dexamethasone (80). The use of anti-VEGF and dexamethasone agents has increased substantially since their introduction and they are the first-line therapy in conditions such as wet-AMD, CRVO and many other acquired retinal diseases. Even though the usage has increased immensely in recent years, there are few studies of the anti-VEGF effect on photoreceptor cell function.

Ophthalmic genetics

The genetics underlying IRDs were largely unknown until the 90s. However, in the pivotal study conducted by T. Dryja et al., the authors reported mutation in the rhodopsin (*RHO*) gene as a cause of ADRP (81, 82). The identification of the *RHO*

mutations constitutes a cornerstone of ophthalmic genetics and a revolutionary chapter in the field of ophthalmology, inspiring research, advancement of diagnostic methods, and the evolution of gene therapy. Over time, additional genes have been identified. Currently more than 350 genes are known to be associated with IRDs and approximately 70 genes specifically linked to RP (39).

Aims

The overall thesis aim is to enhance the understanding of the relationship between retinal structure, as measured by OCT, and retinal function, as measured by ERG, in acquired and inherited retinal degenerative diseases. For this purpose, we employed standard technologies, such as OCT and ERG, to assess retinal structure and function. These techniques allowed us to systematically evaluate the retina in patients with diverse pathologies, including IRDs and acquired retinal diseases. By employing these established methods, we aimed to investigate how variations in retinal structure correlate with functional outcomes.

The specific aims were:

Paper I   To assess structural changes in the macular region of eyes with RP, determine the macular shape and identify characteristics influencing macular structure.

Paper II   To evaluate the long-term changes in the macular curvature in eyes with RP and to determine factors associated with the macular shape.

Paper III   To describe the ophthalmological and genetic features of Danon disease, with a focus on the correlation between retinal structure and function for early diagnosis of this rare, life-threatening systemic disorder.

Paper IV   To evaluate the long-term outcome in retinal function together with macular structure in CRVO eyes treated with series of anti-VEGF and dexamethasone intravitreal injections, and to compare the results with untreated CRVO eyes.

Methods

Ethics

All subjects participating in this thesis were given information about the studies and that participation was voluntary. All the subjects gave their informed written consent before participating. Patient records were anonymised and de-identified prior to analysis. The protocol for the studies and procedures adhered to the tenets of the Declaration of Helsinki. Studies I and II were performed at Nagoya University hospital, Nagoya, Japan and additionally approved by the Institutional Review Board/Ethics Committee of the Nagoya University Hospital, Nagoya, Japan. Studies III and IV were conducted at Skåne University Hospital, Lund, Sweden and approved by the Ethics Review Authority in Sweden.

Safe data management is of fundamental importance. When DNA testing is performed, we focus exclusively on ophthalmological diseases, which are currently linked to around 350 causative genes. DNA testing is offered to patients when its clinically relevant, after explaining the purpose and implications of genetic testing, leaving the decision to the patient. At the ophthalmology department in Lund University, we have several years' experience in handling genetic data and adhere to the tenets of the declaration of Helsinki for medical research.

Ophthalmological examinations

All studied patients underwent regular clinical ophthalmological examination with slit-lamp inspection of the anterior segments (including cornea, anterior chamber, iris and lens). And, after pupil dilation, ophthalmoscopic examination of the posterior segment (including vitreous, macula, optic nerve, retina and retinal vessels). Furthermore, best corrected visual acuity (BCVA) was measured. In papers I and II, VA was performed by using a Japanese standard visual acuity chart and the results were converted to the logarithm of the minimum angle of resolution (logMAR) for statistical analysis. Counting fingers, hand motion, light perception, and no light perception were designated as 1.85, 2.30, 2.80, and 2.90 logMAR units, respectively (83).

In paper III, VA was evaluated using decimal letter charts, and in paper IV, VA measured with decimal letter chart was converted to early treatment diabetic study (ETDRS) letter score for statistical analysis. Additionally in paper IV, inspection of the trabecular meshwork and evaluation of the anterior chamber angle (gonioscopy) were performed with a 2-mirror gonioscopy lens (Sussman) after corneal anaesthesia. The anterior chamber angle was characterised as open, narrow or closed.

Electrophysiological examination

Full-field electroretinography (ffERG)

FfERG measures the total function of the retina. During an ffERG examination, the equipment generates a light stimulus at different wavelengths and light intensities to elicit separate rod- and cone responses as well as combined rod-cone responses. The electrophysiological examinations were performed using a standard protocol recommended by the ISCEV with a few minor modifications listed, given below in papers III and IV. An extended ISCEV protocol was performed in papers I and II.

The ffERG in papers I and II were performed at Nagoya University Hospital, Japan, with full-field scotopic flash ERG elicited by a stimulus strength of 300 cd-s/m^2 (PE300; TOMEY, Nagoya, Japan). The pupils were dilated with tropicamide 0.5% and phenylephrine hydrochloride 0.5%. The eyes were dark-adapted for 40 minutes. After that, the eyes were anesthetised with oxybuprocaine and a Burian-Allen bipolar contact lens electrode (Hansen Ophthalmic Development Laboratories, Iowa City, IA, USA) was applied to the cornea along with a ground electrode on the forehead. The electrical response from the retina was recorded and displayed as a wave pattern. This ffERG testing adheres to the ISCEV extended protocol, which describes ERG stimulus-response series with increased flash strengths. It is referred as 'luminance response' or 'intensity response' and the stimulus should be referred to as DA30. In clinical practice a higher flash strength might be needed for example if the pupils are smaller (84, 85). In papers III and IV, the ffERGs were performed at Lund University, Lund, Sweden, with an Espion E2 analysis system (Diagnosys, LLC, Lowell, Massachusetts, USA) according to the ISCEV standard protocol with minor modifications. Prior to retinal examination, the eyes were dilated using cyclopentolate 1% and phenylephrine 10% and the patients were dark-adapted for 40 minutes. After dark adaptation, the eyes were anesthetised with oxybuprocaine 0.5%, and a Burian-Allen contact lens electrode was applied to the cornea with a ground electrode on the forehead. The electrical response was recorded and shown as a wave pattern.

Multifocal electroretinography (mfERG)

MfERG measures electrical responses from the central part of the retina, in the macular region, corresponding to the central 50 degrees of the visual field.

The mfERG was performed in paper III and recorded with a Visual Evoked Response Imaging System (VERIS Science 6; EDI, San Mateo, USA) according to the ISCEV standard protocol. The stimulus matrix consists of 103 hexagonal components that alternate between black and white at a sequence of 75 Hz at a screen 30 cm from the patients' eyes. Prior to examination, the pupils were dilated with cyclopentolate 1% and phenylephrine 10%. When the pupils were fully dilated, the cornea were anesthetised with oxybuprocaine 0.5%, and a Burien-Allen bipolar ERG contact lens electrode was applied to the eye with a ground electrode on to the forehead. The electrical response is shown as a pattern.


Electro-oculography (EOG)

An EOG recording is an electrophysiological test used to measure electric potential changes between the anterior part of the eye (cornea) and the posterior part (retina) during eye movements. It measures the function and health of the RPE. The eye functions like a dipole with the cornea being electrically positive and the retina negative. When the eye moves, the electrical potential changes and can be recorded using skin electrodes. The EOG recording was performed in paper III using Espion E2 analysis system (Diagnosys, LLC, Lowell, Massachusetts, USA). First, the pupils were dilated with cyclopentolate 1% and phenylephrine 10%. Two skin electrodes were placed at the canthus of each eye to record the electrical activity. The patient sits in a dark room for 20 minutes while the activity is recorded; this is called the 'dark trough'. Then the eyes are exposed to bright light for 10 minutes and the activity is recorded again during photopic conditions. This part of the recording is named the 'light peak'. The light peak/dark trough was calculated by the Espion analysis system program and results were shown as an Arden Ratio (AR). An AR above 1.8 indicates a healthy RPE and an AR below 1.6 indicates a damaged RPE and suggests retinal disease (86). This method is less commonly used today due to advances in retinal imaging techniques, such as OCT and genetic analysis.

Optical coherence tomography (OCT)

OCT is an advanced imaging technique that uses light to create detailed cross-sectional images of the retinal cell layers (Figure 11). It is non-invasive and has a pivotal role in monitoring retinal morphology, disease progress and treatment effectiveness over time. Three types are used in these studies: namely spectral domain OCT (SD-OCT), a rapid scan that captures data from all depths

simultaneously; swept source OCT (SS-OCT), which uses a laser that allows deeper imaging of the vascular layer (choroid) below the retina; and SS-OCT-angiography (SS-OCT-A), which builds on the principles of SS-OCT and enables non-invasive visualisation of retinal and choroidal vasculature (87) (Figure 12).
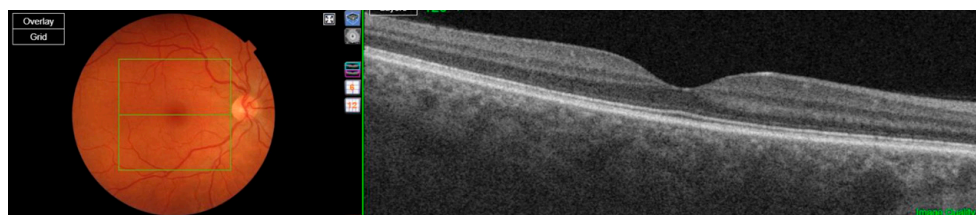
Figure 11. Fundus photo and optical coherence tomography scan of a healthy human retina.
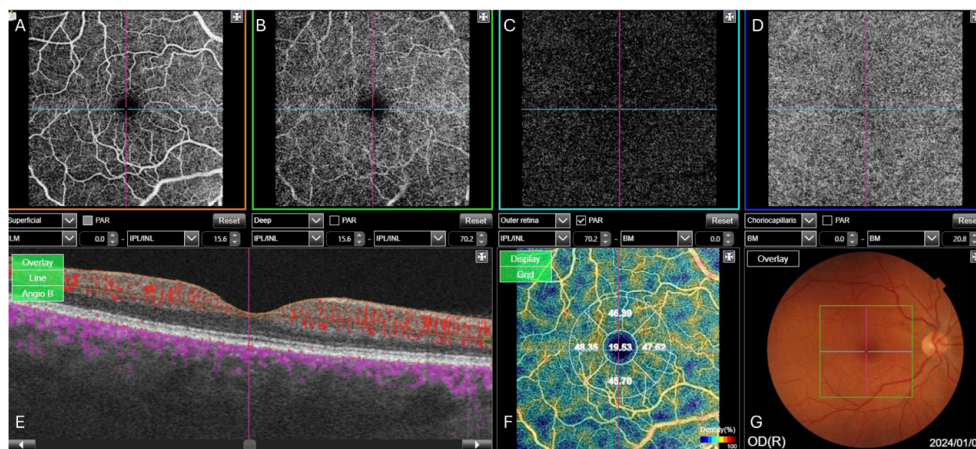
Figure 12. Optical coherence tomography angiography scan of a normal human retina. (A) shows the normal superficial inner retina (superficial retinal plexus). (B) presents the deep inner retina (deep retinal plexus). (C) shows the normal outer retina. (D) shows normal choriocapillaris/choroidea. (E) shows the Angio B scan. (F) shows a vascular density map of the deep retinal slab (cross sectional volume). (G) shows a fundus photo.

For papers I and II, we used the SD-OCT (Heidelberg Engineering, Heidelberg, Germany). The images were of 9-mm radial scans. Horizontal and vertical scans were performed. For papers III and IV, the OCT was performed using SD-OCT-1000, version 3.00 software or a SS-OCT; DRI OCT Triton Plus, Swept Source OCT instrument with multi-model fundus imaging (Topcon, Tokyo, Japan). The macular scan option was used for all scans in this study, centered on the fovea and covering an area of 6 × 6 mm. Additionally, in paper III, the SS-OCT-A was performed using the DRI OCT Triton Plus, Swept Source OCT instrument with multi-model fundus imaging (Topcon, Tokyo, Japan).

Curvature maps made from SD-OCT

A new software was developed by Kyoto and Nagoya Universities in Japan in 2014, to evaluate the posterior pole in myopic eyes with staphyloma (mapping of fundus curvature). The new software using MATLAB (The MathWorks, Inc., Natick, MA, USA) calculated the posterior pole curvatures based on OCT images and constructed a curvature map. In papers I and II, we used this novel method. Our patients had SD-OCT (Heidelberg Engineering, Heidelberg, Germany) of 9-mm radial scans recorded on the horizontal and vertical axis. Each OCT image was adjusted to correct for the difference in pixel resolution in the transverse and longitudinal directions. Bruch's membrane line was plotted from 0 to 8000 μm every 200 μm and with approximately 17-18 plots. With 12 plots from the centre of the fovea on both sides, 1 point in the fovea, 5 points on the nasal side and 6 on the temporal side (Figure 13A). The software calculated the curvature from the marked 12-points by using cubic spline interpolation (yellow and red lines in Figure 13B). The software further calculated the curvatures from 3 mm from the central fovea on the temporal and nasal sides (red line), in total 6 mm. The result was presented as mean macular curvature index (MMCI). A negative (-) MMCI value indicated a concave shape, a positive (+) value indicated a convex shape and a zero (0) indicated a flat macular shape (88).
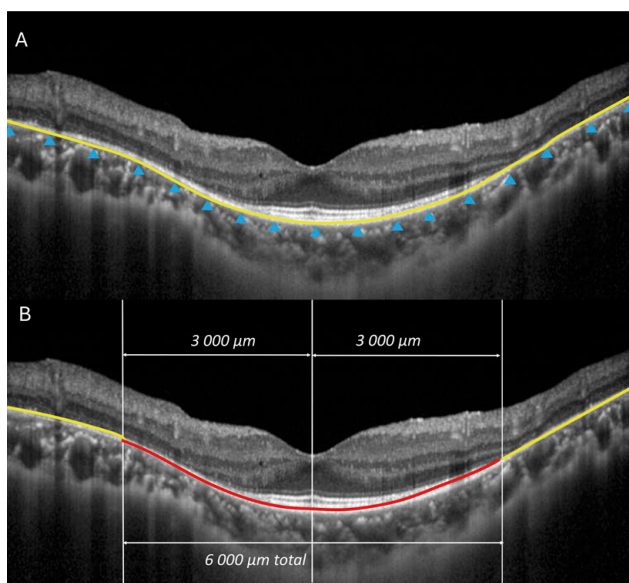
Figure 13. Mean macular curvature index (MMCI) measurement based on OCT images from a retinitis pigmentosa patient. (A) shows plotting of Bruch's membrane line with 17 points. (B) shows the software calculating the MMCI curvature from the red line, central marked 12 points. With permission from: Meinert M et al. Investigation of macular curvature in patients with retinitis pigmentosa using curvature maps constructed from optical coherence tomography. Poster presented at: ARVO 2019 Annual meeting; April 28 - May 2, Vancouver, B.C.

Ellipsoid Zone measurement made from SD-OCT

EZ is the second highly reflective band on the OCT scans and corresponds to the photoreceptor inner segments. In papers I and II, the EZ measurement was performed with SD-OCT (Heidelberg Eye Explorer software, Heidelberg Engineering, Heidelberg, Germany). EZ width was measured between the borders where the EZ band met the upper surface of RPE using the built in calibre. If the EZ width exceeded the OCT scan border of EZ, the width was set at the edge of the OCT scan (36) (Figure 14).
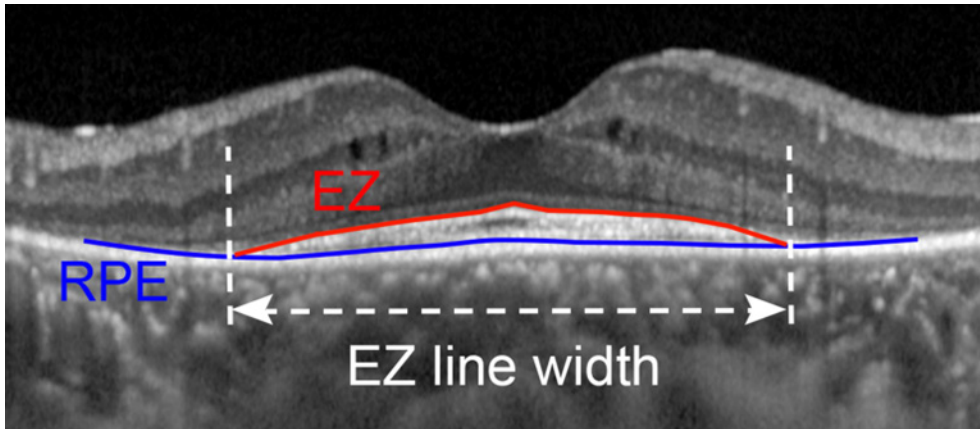
Figure 14. Ellipsoid zone width measurement in an OCT scan of a patient with retinitis pigmentosa in paper II.

Axial length measurement (AL)

Axial length (AL) was performed in papers I and II at baseline with IOL Master (Carl Zeiss Meditec, Inc., Dublin, CA, USA). This technique uses a non-contact method to measure the length of the eye. Inclusion criteria of the AL were from 21.5 mm to 26.0 mm.

Fundus autofluorescence (FAF)

Fundus autofluorescence (FAF) is an imaging technique that illuminates the retina with a specific light to observe the health of the RPE. This is done by capturing the natural fluorescence emitted by lipofuscin, which is a byproduct of the photoreceptors' metabolism that accumulates in the RPE. If there is an increased metabolism of photoreceptors, this is indicated by a stressed RPE, and the FAF

image presents with increased fluorescence (hyperautofluorescence). If there is degeneration and atrophy of the RPE, the image presents with a decreased fluorescence (hypoautofluorescence) (89, 90).

In paper III, we performed FAF with a Topcon TRC-50DX retinal camera with a 535-585 nm excitation bandpass filter and a 605-715 nm barrier bandpass filter (Topcon, Tokyo, Japan).

Fluorescein angiography (FA)

In paper III, we performed FA, a diagnostic imaging technique to assess retinal and choroidal circulation through intravenous injection of the dye with sodium fluorescein. The dye remains primarily bound to proteins (80%) and the rest (20%) is unbound. If the RPE is healthy, it blocks the dye; however, the choriocapillaris allows it to diffuse freely. Fundus images are taken with a specialised camera with filters, initially with blue wavelength spectrum (465-490 nm), which excites the free dye molecules and emits florescence at 520-530 nm (yellow-green spectrum) and this fluorescence is recorded. The dye first reaches the choroid (10-15 s), then the retinal arteries (16 s), then spreads to the capillaries and enters the veins (approximately 17-20 s), then completely fills the venous system (30 s). Common pathological findings include hyperfluorescence and refer to leakage seen in, for example, neovascularisations. Hypofluorescence (reduced fluorescence) is due to blockage of the dye, for example haemorrhage or vascular filling defects. Images are captured with short time intervals to map the retinal circulation (91).

Indocyanine green angiography (ICG)

Indocyanine green angiography (ICG) is another diagnostic imaging technique like FA, but it evaluates choroidal circulation, and especially the deeper choroid plexus, which cannot be visualised through FA. The ICG dye binds in 98% to plasma proteins and is therefore prevented from leaking out of normal choroidal vessels. ICG dye fluoresces at near 790-805 nm, near infrared light. This allows deeper penetration and allows better visualisation of blockage such as haemorrhages, pigments or tumours. The dye reaches the choroidal vascularisation within 10-20 seconds and common pathological findings are seen as hypo or hyper fluorescent. Early mid-phase (1-3 min) shows more prominence of choroidal veins. In late mid-phase (3-15 min) the choroidal vessels and abnormal vasculatures are visible; in late phase (15-45 min) the dye persists in abnormal choroidal vessels, for example in the cases of central serous chorioretinopathy (92).

Humphrey Field Analyser (HFA)

The Humphrey Field Analyser (HFA) was used in paper III. The HFA is an automated perimetry device and the predominant technique for assessing the function of the visual field. The HFA consists of software programs that help the clinician to determine whether a patient's visual field result is comparable with a normal and age- matched result (93).

Molecular genetic testing

Genetic analysis was performed in paper III on genomic DNA from peripheral blood using Next Generation Sequencing (NGS) Blueprint Genetics (BpG) Core Cardiomyopathy Panel (version 1.1, updated May 6, 2014) consisting of the *LAMP2* gene and 71 other genes associated with cardiomyopathy.

Results

Paper I - Steeper macular curvature in eyes with non-highly myopic retinitis pigmentosa

In this cross-sectional study, we evaluated the structural alteration of the posterior pole (staphyloma) in the macular region in eyes with RP and in healthy eyes, in order to determine if there is any difference between the two groups. The study included 143 right eyes of RP patients and 60 right eyes of healthy individuals that served as controls. The clinical parameters of the RP and controls are presented in Table 1.

Table 1. Clinical parameters of retinitis pigmentosa patients and healthy controls. NA= not available.

Parameter	Retinitis pigmentosa patients (n=143)	Control (n=60)	P-value
Age, years, mean $\pm$ SD	48.62 ± 16.26	47.30 ± 17.7	0.57
Axial length, mm, mean $\pm$ SD	23.83 ± 1.02	24.08 ± 0.93	0.074
Curvature Mean Macular Curvature Index (MMCI) x 10 $^{-5}$ μm $^{-1}$ mean $\pm$ SD	- 13.73 ± 9.63	- 6.63 ± 5.63	**<0.001***
Ellipsoid zone width, μm	2227.29 ± 2269.09	NA	

Using a novel technique derived from OCT scans, developed by Miyake et al. (88), we assessed the macular curvature in horizontal OCT scans in both groups (Figure 15).
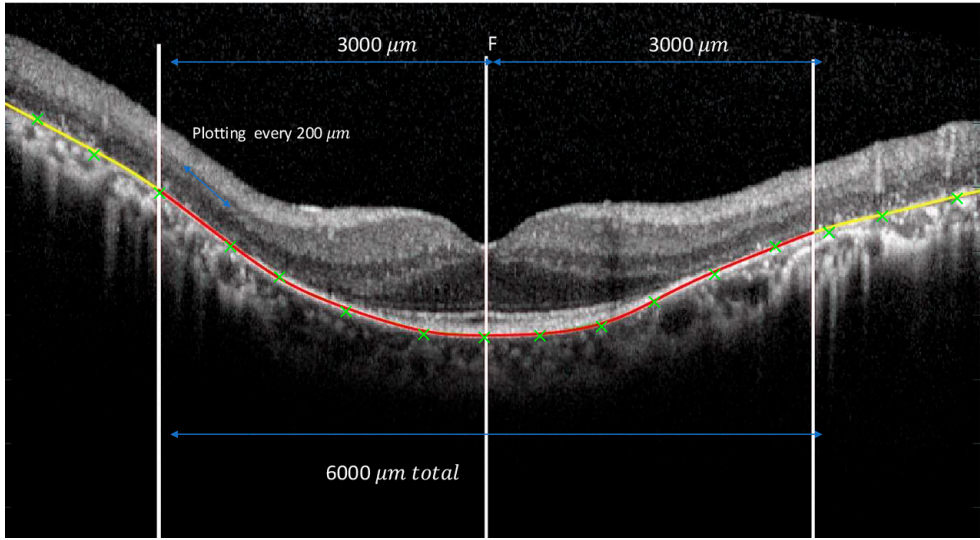
Figure 15. Mean Macular Curvature Index measurement based on ocular coherence tomography in retinitis pigmentosa patient in paper I.

The result was presented as the mean macular curvature index (MMCI). The MMCI for the control eyes was $-6.63 \pm 5.63 \times 10^{-5}$ μm^{-1} and for the RP eyes was $-13.73 \pm 9.63 \times 10^{-5}$ μm^{-1} (p= < 0.001), indicating that the macular curvature was more steeply concave in the RP eyes. Further, we examined which factors were significantly associated with MMCI and found that RP and AL were significant independent factors for predicting the MMCI. This suggested that the category of RP and longer AL were significantly correlated with lower MMCI values, thus steeper macular curvature. Next, we analysed the correlation of MMCI and several clinical parameters and found a low correlation coefficient with AL (r = -0.24, p = 0.004) and age (r = 0.20, p = 0.016). Further, we performed an analysis to determine whether there is a correlation between photoreceptor degeneration (EZ width) and MMCI values. We found a non-linear effect between the two parameters. Therefore, we conducted additional analyse by dividing the EZ width into short (0-1311 μm), intermediate (1312-3842 μm) and long (above 3843 μm) EZ groups in RP eyes. The intermediate group presented with a significantly lower MMCI, and we also found that the macular curvature was steeper in eyes with EZ width greater than 2200 μm.

Paper II - Longitudinal changes of macular curvature in patients with retinitis pigmentosa

This retrospective study is a follow-up of paper I, where we evaluated the longitudinal data of macular curvature in the RP eyes and investigated associated factors that could affect the macular shape. The 107 patients were included from the dataset of paper I (Table 2). The oldest and newest OCT scans, both in horizontal and vertical axis of the macular curvature, were analysed at least 1 year apart.

Table 2. Clinical characteristics including number of patients, age, axial length and observation time of retinitis pigmentosa patients at baseline.

Characteristics at baseline in retinitis pigmentosa patients		Gender distribution
Patients (n=107)	Male (n=44)	Male = 41%
	Female (n=63)	Female = 59%
Age, years, mean ± SD	45.9 ±16.2	
Axial length, mm, mean ± SD	23.80 ± 1.05	
Observation time, years, mean ± SD	3.4 ± 1.4	

During the mean observation time of 3.4 ± 1.4 years (mean ± SD) both the VA and EZ width decreased significantly ($p < 0.001$ and $p < 0.0001$, respectively).

Table 3. Clinical data at baseline and follow-up in RP eyes. BCVA = best corrected visual acuity, MAR = minimum angle of resolution, MMCI=Mean Macular Curvature Index, EZ = Ellipsoid Zone, NA = not available, *Statistical significance ($p <0.05$).

Clinical data at baseline and follow-up	Baseline	Follow-up	P-value
BCVA (logMAR) mean ± SD	0.22 ± 0.30	0.29 ± 0.35	**<0.001***
Vertical Mean Macular Curvature Index MMCI ($x10^{-5}\mu m^{-1}$) mean ± SD	-15.47 ± 9.52	-16.36 ± 9.78	**0.008***
Horizontal Mean Macular Curvature Index MMCI ($x10^{-5}\mu m^{-1}$) mean ± SD	-14.38 ± 9.09	14.59 ± 9.22	0.36
EZ width at vertical scan (µm) mean ± SD	2158 ± 2136	1883 ± 2100	**<0.0001***
Axial Length (mm) mean ± SD	23.80 ± 1.05	NA	NA

The MMCI decreased significantly as seen in the vertical OCT scans, from -15.47×10^{-5} μm^{-1} to -16.36×10^{-5} μm^{-1} ($p = 0.008$) (Table 3). This indicates that the macular curvature became steeper in the vertical axis during the study time. However, no significant changes were found in the horizontal macular curvature on the OCT scans ($p = 0.36$). Further, we investigated the association between the

vertical MMCI and the EZ width. The EZ width decreased significantly during the study time, although it changed independently from the MMCI.

However, knowing the result from paper I, where the macular curvature became steeper in the RP eyes with EZ greater than 2200 μm, we divided the RP-eyes according to EZ width. The mild group with EZ width >2000 μm, moderate 0-2000 μm, and severe 0 μm. Only the RP-eyes in the mild group presented with a steeper macular curvature in the vertical axis (p =0.011), while moderate and severe groups had non-significant change in the MMCI during the study time (Figure 16). The OCT scans and fundus photos of three representative RP patients at baseline and follow-up are presented in Figure 17.
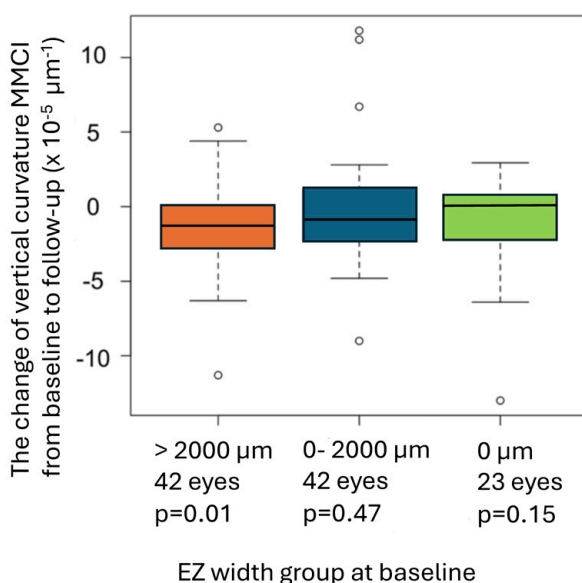
Figure 16. Boxplots presenting the change of the vertical macular curvature index (MMCI) from baseline to follow-up and its correlation to Ellipsoid zone width group at baseline. The mild EZ group showed a significant correlation with vertical MMCI (p= 0.01), meaning that the steepest MMCI was found in patients with preserved EZ width above 2000 μm.
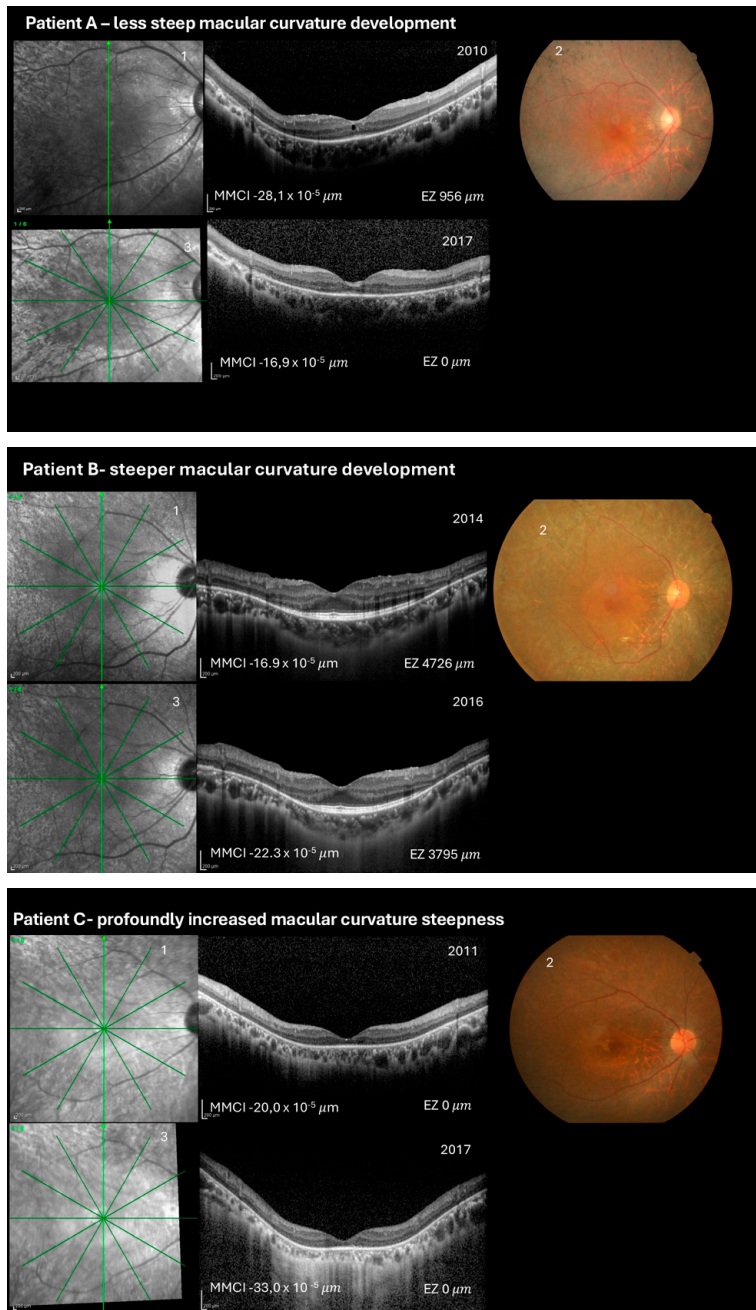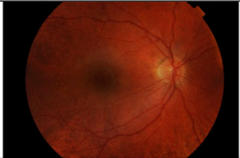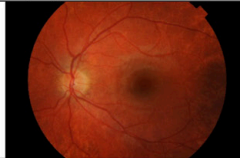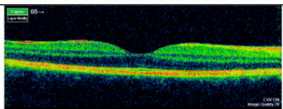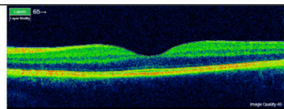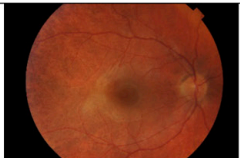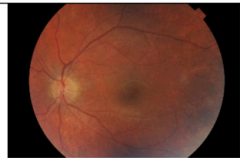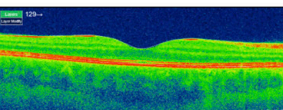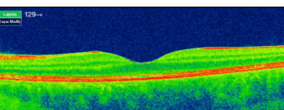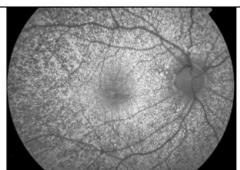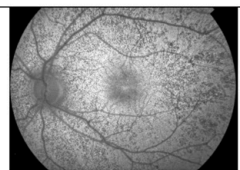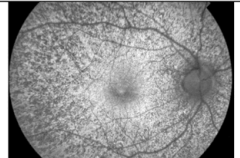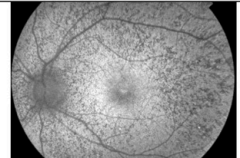
Figure 17. Three representative retinitis pigmentosa cases from paper II showing changes in the Mean Macular Curvature Index (MMCI) during the study time. (1) shows vertical optical coherence tomography (OCT) scans with MMCI and Ellipsoid Zone (EZ) width at baseline. (2) shows fundus photos at baseline. (3) shows vertical OCT scans at follow-up with MMCI and EZ width. Patient A became less steep in the macular curvature during the observation time. Patent B became steeper in the macular curvature during observation time. Patient C became profoundly steep in the macular curvature during observation time.

Paper III - Danon disease presenting with early onset of hypertrophic cardiomyopathy and peripheral pigmentary retinal dystrophy in a female with a de novo novel mosaic mutation in the *LAMP2* gene
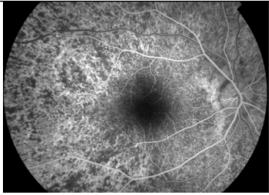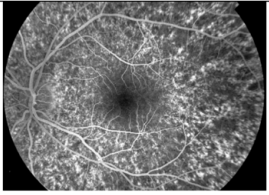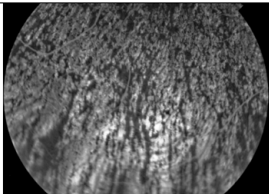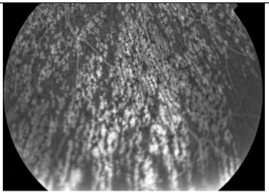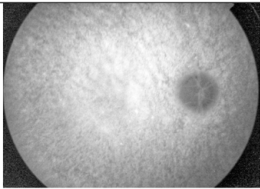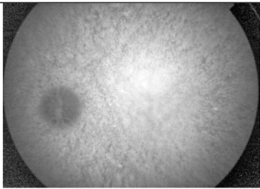
In paper III, we describe the morphology, retinal function and genotype of a patient with Danon disease. The baseline data and 5-year follow-up data were compared.

At age 20 (baseline), the patient presented with a PPRD in both eyes. Colour fundus photographs revealed RPE clumping and atrophy in the macula and periphery. FAF images showed hypofluorescent dots in the macular region. The SD-OCT presented with intact retinal layers and the VA, Humphrey 30-2, mfERG and ffERG were normal at baseline. Genetic analysis was performed using the NGS BpG Core Cardiomyopathy Panel (version 1.1, updated May 6, 2014) consisting of *LAMP2* and 71 other genes associated with cardiomyopathy. Genetic testing identified a *de novo* novel mosaic mutation c.135dupA; p.(Trp46Metfs*10) in the *LAMP2* gene. The *LAMP2* gene variant was mosaically distributed in 16% of peripheral blood lymphocytes and in approximately 30% of the DNA from explanted heart tissue. Immunohistochemical analysis of the heart tissue revealed a pronounced deficiency in the LAMP2 protein in cardiomyocytes; however, many interstitial cells showed presence of LAMP2 protein.

Ophthalmological findings at 5-year of follow-up revealed a more extensive atrophy of the RPE in the peripheral retina on the colour fundus photographs and FAF. The FA revealed numerous small irregular hyperfluorescent spots in the macula and periphery, probably due to transmission defects secondary to RPE atrophy. The ICG showed a similar image. However, these hyperfluorescent dots were mainly located between the macula and the optic nerve head. This observation might reflect build-up of undegraded autophagic material and/or glycogen accumulation in the RPE and/or in the deep inner retina. SD-OCT scans showed no difference between baseline and follow-up. However, the OCT-A showed that the deep inner retina was more irregular, with fewer clearly visible vessels and with the presence of white dots (Figures 18 and 19). At 5-year follow-up, ffERG responses showed an asymmetric reduction between the eyes, with the amplitude of the b-wave rod response being decreased by 29% in the right eye and by 6% in the left eye; however, the amplitudes were still within the normal limits. No changes were observed in VA, OCT, Humphrey 30-2 or mfERG at the 5-year follow-up.

Baseline (20 y)	A	Right eye (OD)	B	Left eye (OS)
Fundus photography				
	OD		OS	
OCT-B	C		D	
	OD		OS	
Follow-up (25 y)	E		F	
Fundus photography				
	OD		OS	
OCT-B	G		H	
	OD		OS	
Baseline (20 y)	I		J	
FAF				
	OD		OS	
Follow-up (25 y)	K		L	
FAF				
	OD		OS	

Figure 18. Colour fundus photographs, optical coherence tomography (OCT) scans and fundus autofluorescence photos (FAF) of a female patient with Danon disease and de novo novel mosaic mutation in the *LAMP2* gene, c.135dupA; p.(Trp46Metfs*10). Colour fundus photography of right and left eye at baseline (A-B) with retinal pigment epithelium (RPE) clumping and atrophy in the macular region and presenting at follow-up (E-F) with more RPE clumping and atrophy. OCT scans at baseline (C-D) and follow-up (G-H) with normal structural appearance in the macula. FAF images of central and paracentral retina presenting at baseline (I-J) with irregular hypoautofluorescence changes secondary to RPE atrophy and loss of normal fundus autofluorescence. FAF at follow-up (K-L) with more widespread hypoautofluorescence in the paracentral and peripheral retina.

	A **Right eye (OD)**	B	**Left eye (OS)**
FA Multiple white dots in central retina			
	OD	OS	
	C	D	
FA Multiple white dots in peripheral retina			
	OD	OS	
	E	F	
ICG Hypo-fluorescent dots in central retina			
	OD	OS	

Figure 19. Fundus fluorescein angiography (FA) and indocyanine green angiography (ICG) performed at baseline in a female patient with Danon disease and de novo novel mosaic mutation in the *LAMP2* gene, c.135dupA; p.(Trp46Metfs*10). (A-D) show FA. (E-F) show ICG. (A-D) demonstrated early phase FA with numerous white dots in both central and peripheral retina. (E-F) show later phase ICG, with numerous small, distinct hypofluorescent dots mainly located between the optic nerve head and macula.

Paper IV - Long-term visual outcome and retinal function with and without intravitreal treatments in eyes with central retinal vein occlusion

In paper IV, we investigated the long-term effects of intravitreal anti-VEGF injections on retinal function, assessed with ERG, and retinal structure, assessed by OCT, in eyes with CRVO. These findings were compared with those from untreated CRVO eyes to evaluate the long-term impact on photoreceptor cell function.

We included 38 eyes from 38 patients diagnosed with CRVO, who underwent an initial ERG (ERGI) within one month prior to treatment and a follow-up ERG (ERGII). Of these, 28 patients with macular oedema received intravitreal treatment and had a follow-up after approximately 3.5 years (mean 42.5 ± 20.3 months) at ERGII. While the 10 patients without macular oedema who remained untreated had a follow-up after at approximately 5.4 years (mean 64.9 ± 22.0 months) at ERGII. Clinical follow-up data were also collected at final visit between 6.2 years in treated and 7.4 years in non-treated patients after CRVO diagnosis (Table 4). The treated group was further subdivided into non-ischemic and ischemic CRVO based on ERG results. The fundus photos and OCT scans of three representative CRVO cases: non-treated, treated (non-ischemic and ischemic) at baseline (ERGI) and at follow-up (ERGII) are presented in Figure 20. Additional parameters, including VA, OCT, IOP and associated ocular and systemic diseases were reported.
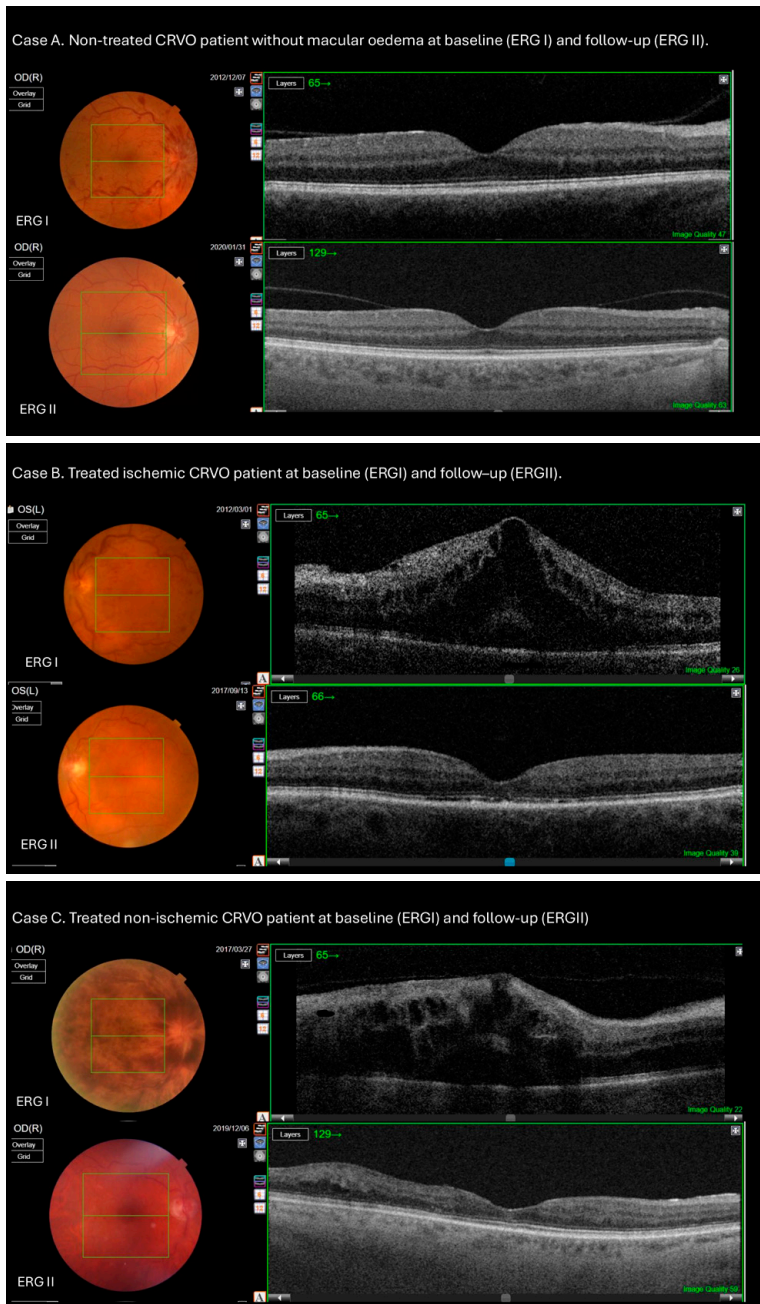
Figure 20. Fundus photos and optical coherence tomography scans of three representative cases of central retinal vein occlusion (CRVO) from the present study at baseline (ERGI) and follow-up (ERGII). Case A; non-treated CRVO patient without macular oedema at ERGI and ERGII. Case B; treated ischemic CRVO patient with presence of macular oedema at ERGI and with resolution of macular oedema at ERGII following anti-VEGF treatment. Case C; treated non-ischemic CRVO patient with macular oedema at ERGI and nearly resolved macular oedema at ERGII following anti-VEGF treatment.

Analysis of the treated and non-treated CRVO groups

The clinical parameters are summarised in Table 4. The BCVA (ETDRS letters) improved significantly in the treated group from ERGI to ERGII and to final visit (p = 0.002 and p = 0.026, respectively). In contrast, the non-treated group showed a non-significant improvement in BCVA across the same time. The mean central foveal thickness (CFT) decreased significantly in both groups from ERGI to ERGII and from ERGI to final visit (treated group: p <0.001 and <0.001; non-treated group: p < 0.002 and p = 0.004, respectively). Notably, baseline CFT (ERGI) differed significantly between the treated (684 ± 172.2 μm) and non-treated (375.3 ± 114.8 μm) groups.

Table 4. Clinical parameters of treated and non-treated Central Retinal Vein Oclussion (CRVO) groups: age, Best Corrected Visual Acuity; (BCVA, ETDRS Letters); Central Foveal Thickness (CFT) and follow-up period in months and years at baseline (ERGI), follow-up (ERGII) and final visit. p_1- Mann-Whitney U-test; used for comparisons between groups; p_2- Wilcoxon signed rank test (baseline ERGI vs follow-up ERGII) used for comparisons within each group; p_3- Wilcoxon signed rank test (baseline ERGI vs final visit). * Statistically significant.

Clinical parameters		Treated CRVO (n=28)	Non-treated CRVO (n=10)	p_1
Age (years) mean ± SD		69.8± 10.6	66.5 ± 12.4	
BCVA (ETDRS letters) mean ± SD	ERGI	47.4 ± 19.2	63.1 ± 23.5	**0.022***
	ERGII	60.7 ± 17.8	66.2 ± 23.6	
	Final visit	58.1 ± 22.6	67.1 ± 21.2	
	p_2	**0.002***		
	p_3	**0.026***		
Central foveal thickness (μm) mean ± SD	ERGI	684.4 ± 172.7	375.3 ± 114.8	**<0.001***
	ERGII	262.1 ± 113.0	229.3 ± 56.0	
	Final visit	220.1 ± 58.0	240.4 ± 67.8	
	p_2	**<0.001***	**<0.002***	
	p_3	**<0.001***	**0.004***	
Follow-up period months (approximal years) mean ± SD	ERGII	42.5 ± 20.3 (3.5)	64.9 ± 22.0 (5.4)	**0.011***
	Final visit	74.3 ± 29.3 (6.2)	89.3 ± 18.4 (7.4)	

The ERG results, of the treated and non-treated CRVO groups, are presented in Table 5. Both groups showed a significant reduction in a- and b-wave amplitudes of the combined rod-cone responses from ERGI to ERGII (treated group: p = 0.004 for both and non-treated group: p= 0.037 for both) (Figure 21, 22).

Table 5. Electroretinogram (ERG) results in the treated and non-treated Central Retinal Vein Occlusion (CRVO) groups. Only significant data with p-value <0.05 are presented. Ampl.- amplitude; it- implicit time; p_1- Mann-Whitney U-test, used for comparisons between groups; p_2 and p_3- Wilcoxon signed rank test baseline (ERGI) vs follow-up (ERGII), used for comparisons within each group regarding amplitude (p_2) and implicit time (p_3). There is a significant decrease in a- and b-wave amplitudes of combined rod-cone response from ERGI to ERGII in both the treated and non-treated CRVO groups.

Electroretinogram results			Treated CRVO (n=28)	Non-treated CRVO (n=10)	P_1
Rod response	ERGI	b-wave it	81.4 ± 9.6	77.0 ± 7.5	
	ERGII	b-wave it	75.0 ± 9.2	77.6 ± 5.6	
		P_3	**<0.001***		
Combined rod-cone response	ERGI	a-wave ampl.	169.9 ± 58.7	176.5 ± 68.5	
		a-wave it	21.7 ± 3.3	19.2 ± 2.1	**0.030***
	ERGII	a-wave ampl.	136.8 ± 51.8	132.9 ± 36.6	
		a-wave it	19.2 ± 3.1	19.5 ± 3.7	
		P_2	**0.004***	**0.037***	
		P_3	**<0.001***		
	ERGI	b-wave ampl.	331.6 ± 116.1	307.3 ± 103.4	
	ERGII	b-wave ampl.	271.1 ± 87.2	250.2 ± 71.7	
		P_2	**0.004***	**0.037***	
Single-flash response	ERGI	a-wave it	16.9 ± 1.7	15.4 ± 1.7	**0.044***
	ERGII	a-wave it	14.5 ± 1.5	15.5 ± 1.3	
		P_3	**<0.001***		
	ERGI	b-wave ampl.	62.5 ± 24.4	55.6 ± 21.5	
	ERGII	b-wave ampl.	51.7 ± 19.5	52.6 ± 18.9	
		P_2	**0.035***		
30Hz flicker response	ERGI	b-wave ampl.	47.3 ± 23.4	40.5 ± 14.5	
		b-wave it	37.3 ± 3.4	36.0 ± 4.4	
	ERGII	b-wave ampl.	41.2 ± 20.4	32.8 ± 13.2	
		b-wave it	34.8 ± 3.5	33.6 ± 3.8	
		P_2		**0.014***	
		P_3	**<0.001***	**0.041***	
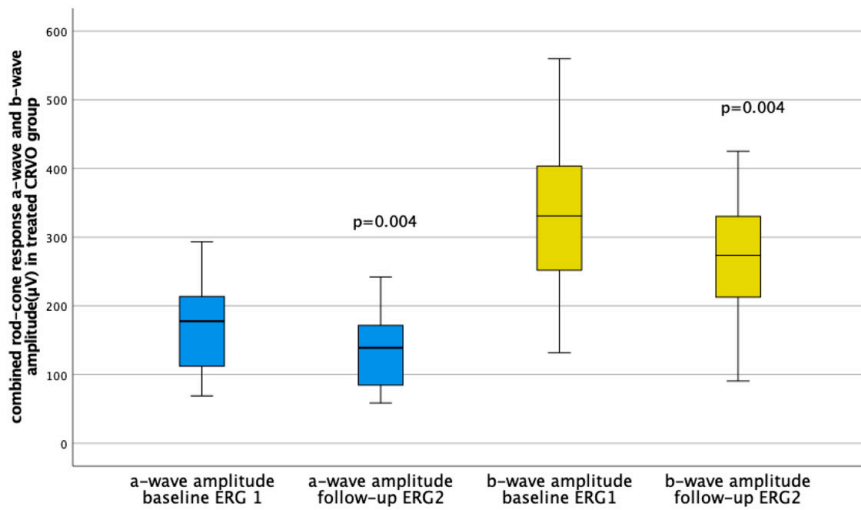
Figure 21. Boxplots presenting Electroretinogram (ERG) results in the treated central retinal vein oclussion group with a significant decrease of a-wave (blue) and b-wave (yellow) amplitudes of combined rod-cone response from baseline ERG1 (ERGI) to follow-up ERG2 (ERGII).

Figure 22. Boxplots presenting Electroretinogram (ERG) results in the non-treated central retinal vein occlusion group, with a significant decrease of a-wave (blue) and b-wave (yellow) amplitudes of combined rod-cone response from baseline ERG1(ERGI) to follow-up ERG2 (ERGII).

Regarding implicit times, the treated group showed a significant shortening in the b-wave of the rod- and the 30 Hz flicker responses (p < 0.001 and p < 0.001, respectively), as well as in the a-wave implicit times of combined rod-cone and

single-flash ERG responses (p < 0.001 and p < 0.001, respectively). In the non-treated group, a significant shortening was observed in the b-wave implicit time of the 30 Hz flicker response (p = 0.041).

The most common ocular complications in both groups were glaucoma and ocular hypertension. The most common systemic conditions in both groups were hypertension and a combination of hypertension and hyperlipidaemia.

Subgroup analysis of the treated non-ischemic and ischemic CRVO groups

BCVA (ETDRS letters) improved significantly in the ischemic group from ERGI to ERGII (p = 0.023), while the non-ischemic group showed a non-significant improvement (Figure 23). The ffERG results of the treated non-ischemic CRVO group showed a significant reduction in a- and b-wave amplitudes of the combined rod-cone response from ERGI to ERGII (p = 0.008 and p = 0.027, respectively) (Figure 24). The treated ischemic group showed a non-significant reduction in a- and b-wave amplitudes of the combined rod-cone response from ERGI to ERGII.
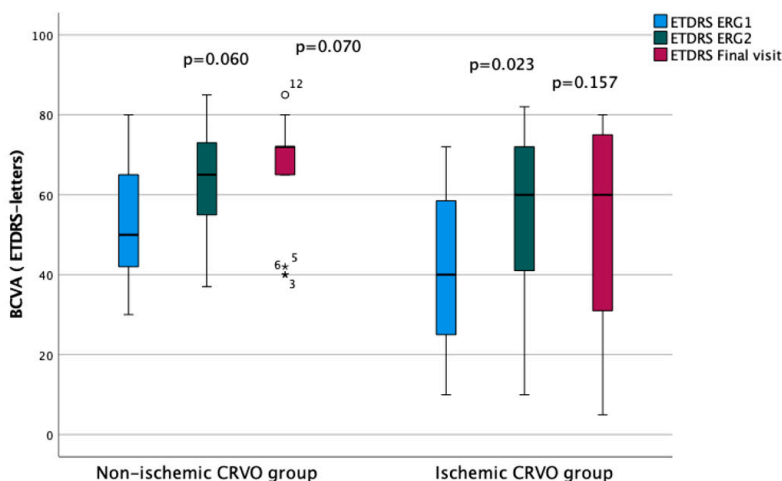
Figure 23. Boxplots with subgroup analysis of the treated ischemic and non-ischemic central retinal vein occlusion (CRVO) groups and the changes of best corrected visual acuity (ETDRS letters) from baseline ERG1 (ERGI), follow-up ERG2 (ERGII) and final visit. Only the ischemic CRVO group showed a significant improvement from baseline to follow-up (p = 0.023).
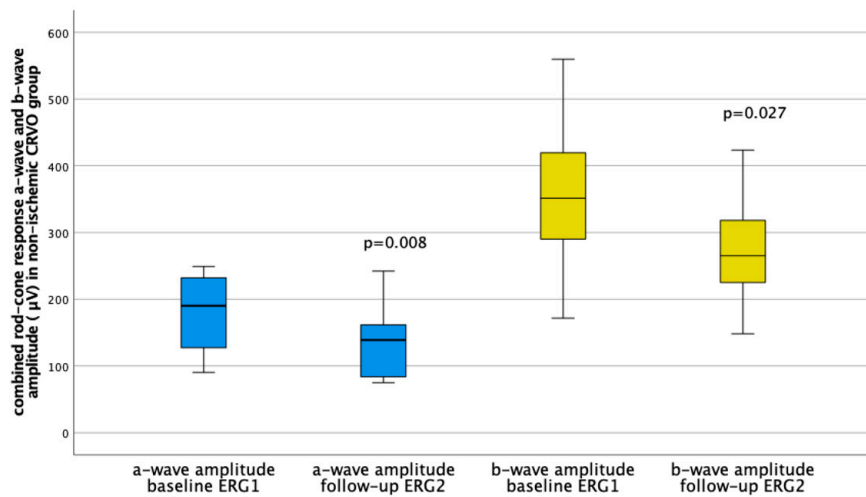
Figure 24. Boxplots presenting Elecretroretinogram (ERG) results in the subgroup analysis of the treated non-ischemic Central Retinal Vein Occlusion (CRVO) group with a significant decrease of a-wave (blue) and b-wave (yellow) amplitudes of combined rod-cone response from baseline ERG1 (ERGI) to follow-up ERG2 (ERGII).

Discussion

The overall aim of this thesis was to advance the understanding of retinal degenerative diseases by assessing the changes of retinal morphology and function (papers I, II and IV) and to determine the relationship between phenotype and genotype (paper III). Across the four papers, retinal structure and function were evaluated using objective and advanced imaging techniques, such as OCT, and electrophysiological methods.

Structural changes in retinal degenerative diseases - Papers I and II

Structural changes of the posterior part of the eye, including staphyloma, have been observed in pathological and high myopia, defined as refractive error of at least -6 dioptres (D) or less or an axial length of 26.5 mm or more. Although such changes are very rare in non-highly myopic eyes (94). At the same time, there is limited knowledge about the occurrence and characteristics of staphyloma and posterior pole changes in the adult population with retinal degenerative diseases, such as RP (50).

In papers I and II, we used a novel imaging method for posterior pole and macular curvature measurements, derived from OCT, originally developed for analysing highly myopic eyes (88); the MMCI. To the best of our knowledge, papers I and II are the first to evaluate morphological differences in the macular curvature of the posterior pole in detail in patients with RP compared to healthy eyes. At the time of publication in 2020, few accurate methods existed for assessing the detailed structure of the macular curvature. Conventional imaging modalities, such as computed tomography, magnetic resonance imaging, widefield fundus imaging (e.g., Optos), and ocular ultrasound, provided limited resolution and were insufficient for capturing the subtle morphological characteristics of the macula. The OCT-based method applied in papers I and II offered enhanced precision and reproducibility, establishing a new approach for studying posterior segment changes in retinal degenerative diseases.

In paper I, we performed a cross-sectional analysis and identified a high prevalence of steep macular curvature in non-highly myopic RP eyes compared to control eyes.

AL was found to be an independent predictor of macular curvature steepness, with less influence from age or sex. These findings align with previous population-based studies on staphyloma formation in high myopia (94). We hypothesised that the macular curvature steepness, as measured by MMCI, would correlate with photoreceptor degeneration, and specifically that the curvature would become steeper and more concave with severe EZ degeneration. Surprisingly, MMCI appeared to change independently of EZ width. Further analysis showed that the steepest macular curvature occurred in RP eyes with relatively preserved EZ width (approximately 2200 µm), indicating that the curve changes occur independently of the degree of photoreceptor degeneration.

In paper II, we conducted a longitudinal analysis of macular curvature changes in 107 RP eyes over a mean follow-up time of 3.4 years. OCT scans were evaluated along the vertical and horizontal axes. Our results showed a significant increase in curvature steepness along the vertical axis, with no significant change along the horizontal axis. Interestingly, eyes with preserved EZ width (> 2000 µm) classified as 'mild' RP in our study exhibited a more pronounced steepening of the macular curvature over time. However, once again, no direct correlation was found between curvature steepness and EZ width. This supports the conclusion from paper I that these structural changes occur independently from EZ degeneration. A noteworthy finding was that the change to a steep macular curvature in the longitudinal study, was only significant in the vertical axis, and non-significant in the horizontal axis of the curvature. One possible explanation for this is that, in highly myopic eyes with staphyloma, the superior and temporal retina are more prone to deformation (95). Additionally, the presence of the optic disc and optic canal may restrict the curvature changes along the horizontal axis. It is also possible that horizontal changes progress too slowly to be detected within the duration of the study. It is important to note that not all RP eyes exhibited increased steepness. In 69 out of 107 patients (65%), the macular curvature became steeper, while in 38 patients (36%) it became less concave. In five patients, significant macular oedema was observed at baseline, contributing to a steeper initial macular curvature. Following resolution of the oedema, the curvature became markedly less concave. Macular oedema, which occurs in approximately 10-40% of RP eyes and is a known complication (96, 97) may have confounded the curvature measurements.

Overall, these structural findings suggest that the posterior pole alterations in RP are likely linked to broader retinal structure changes. Although RP is primarily a photoreceptor disease, reports show that it also affects the inner retinal layers, including bipolar and Müller cells, particularly as the disease progresses. Recently, Yoon et al. investigated longitudinal changes in the retinal and choroidal microstructure of the macula in 69 RP patients and compared it with healthy age-matched controls (98). Notable reductions were recorded in the thickness of the IPL, ONL and inner segment ellipsoid at the moderate stage, alongside the NFL and IPL at the advanced stage. Choroidal thickness exhibited a significant decline across all

stages. No changes were observed in the control group. Another plausible contributor to structural changes in the posterior pole is the submacular choroidal thinning, which was reported by Dhoot et al. to occur in both highly myopic and RP eyes (99).

Consideration of the myopic shift

The influence of myopia on our results should be taken in consideration. Myopia is caused by elongation of the eyeball, resulting in light focusing anterior to the retina. It has a multifactorial aetiology involving both genetic and environmental factors (100). Most studies classify non-pathological myopia as less than -6 D, AL less than 26.5 mm, usually developing in childhood or adolescence and stabilising in early adulthood, around the 3rd decade. Pathologic myopia is defined as refractive error of at least -6 D or AL more than 26.5 mm, associated with higher risk of retinal degenerative disease and other complications (101). Papers I and II included only non-highly myopic RP eyes with AL ranging from 21.5 to 26.0 mm (paper I: 23.83 ± 1.02 mm, paper II: 23.80 ± 1.05 mm). In paper I, 16 out of 143 patients (11%) were under the age of 30, including six patients under 20 years of age. In paper II, 15 out of 107 patients (14%) were under 30, with four younger than 20 years of age. Given the known risk of a second myopic shift during the late second or third decades, this could influence the progression of the macular curvature in a lesser extent of the data material.

Genetic and methodological consideration

Xu et al. reported in 2019 about the differences between macular staphyloma types in RP eyes and highly myopic eyes (50). The group drew the conclusion that the macular staphyloma found in the RP eyes belonged to the narrow macular staphyloma type (a deep, narrow, steep over a small diameter, OCT with sharp scleral protrusion and marked thinning in subfoveal choroidal thickness), while the high myopia belongs to the wide macular type (more gentle steepness over a broad area, OCT with shallow protrusion, choroidal thinning present but less focal). This suggests that the mechanism of staphyloma formation in RP may be different and/or multifactorial. Furthermore, genetic factors influencing the posterior pole must be taken into consideration. Staphyloma and coloboma-like changes have been reported in early-onset RP, such as LCA, particularly in genotypes including *NMNAT-1* (45), *IDH3A* (46) and *DHX38* (47) and *CEP-290* (48). Also, X-linked retinitis pigmentosa (XLRP) is frequently associated with high myopia, particularly in female carriers. XLRP accounts for approximately 5-15% of the RP cases (44). The primary gene variant responsible of the majority of XLRP cases is the retinitis pigmentosa GTPase regulator (*RPGR*) gene (102).

At the time of our study, genetic testing had been completed in one of the 143 patients, who carried pathogenic *EYS* gene variants. The lack of genotypic identification for the other patients represents a limitation of our study and highlights the need of genetic analysis in future research to better correlate the genotype with phenotype in order to clarify the molecular mechanisms underlying the structural changes. Another methodological limitation was that in paper I, OCT scans were limited to the horizontal axis, potentially missing vertical changes of the macular curvature, changes that were found to be significant in paper II. Moreover, the lack of AL measurements at follow-up in paper II should be addressed in future studies. Nevertheless, we assessed the refractive status at both timepoints and found no substantial changes. The mean spherical equivalent shifted slightly from -1.53 D at baseline to -1.40 D at follow-up, while the cylindrical values changed marginally from -1.20 D to -1.25 D. These minor differences suggest that myopic progression should not significantly affect the longitudinal analysis.

Several months after the publication of papers I and II, our collaborating Japanese research group extended the investigation into the association between macular curvature and causative genes of RP (103). In this subsequent analysis, using the *EYS* gene as the reference, their analysis revealed a significant association between the *RPGR* gene and MMCI values, even after adjusting for potential confounding factors. In contrast, no significant differences were observed for *USH2A*, *RP1*, or *RP1L1* when compared to the *EYS* gene, suggesting a gene-specific effect on posterior pole morphology.

Linking retinal findings and genetics in rare systemic disease - Paper III

In paper III, we present a young woman with rapidly progressive heart failure whose diagnosis of Danon disease was prompted by detailed retinal examination. Initial referral to the ophthalmology department was based on likely sarcoidosis related eye changes. However, bilateral PPRD was inconsistent with ophthalmic manifestation of sarcoidosis. Structural and functional findings then led us to reconsider the underlying pathology and to reconsider a retinal degenerative disorder with systemic associations. Comprehensive retinal examinations, including structural and functional analysis, revealed pronounced PPRD in both eyes. 5-year follow-up demonstrated a slow progression of retinal degeneration with PPRD, accompanied by asymmetric intraocular reduction in rod and cone responses on ffERG. OCT-A revealed less clearly visible retinal vessels with presence of white dots in the deep inner retina, when compared to age-matched control. Genetic analysis identified a de novo novel mosaic frameshift variant in the *LAMP2* gene c.135dupA; p.(Trp46Metfs*10). Immunohistochemical investigation confirmed a

marked deficiency of LAMP2 protein in cardiomyocytes from patient's explanted heart tissue.

Danon disease, an X-linked lysosomal storage disorder caused by LAMP2 protein deficiency, classically presents with cardiomyopathy, skeletal myopathy and varying neurological and cognitive impairment due to lysosomal dysfunction, leading to the accumulation of autophagic material predominantly in skeletal and cardiac muscles (56). Ocular involvement and retinal abnormalities, although less commonly emphasised, have been reported in up to 69% of affected males and 64% of females with genetically confirmed *LAMP2* gene variants (56). However, the full spectrum and frequency of ocular manifestations remain incompletely characterised due to insufficient ophthalmic follow-up in many cases (53). Our patient exhibited a severe cardiac phenotype, requiring heart transplantation at age 22, approximately a decade earlier than previously reported for female Danon patients. This early onset parallel to other rare cases, including two reported by Hedberg-Oldfors et al. (104), and suggests a possible correlation between genotype, mosaicism level, and disease severity. Despite the severity of the patient's cardiomyopathy, the patient's retinal and neurological symptoms were comparatively mild, highlighting the phenotypic variability of Danon disease, particularly in females with mosaic gene variants.

Genotype-Phenotype considerations and mosaicism

The identified *LAMP2* frameshift variant can have profound effects on the protein structure and function and can be associated with severe Danon phenotypes (105). However, the mosaicism in our patient was detected in 30 out of 180 of the reads, suggesting that the *LAMP2* gene variant was mosaically distributed being found in 16% of the peripheral blood lymphocytes and in approximately 30% of cardiomyocytes in cardiac tissue. This mosaic distribution may have contributed to a milder ocular and neurological involvement. Although the degree of mosaicism could not be directly analysed in the eye, the clinical findings suggest that the level of mosaicism in the retina could be comparable to, or higher, than that found in the lymphocytes, and possibly as high as that in the cardiomyocytes. The immunohistochemical analysis of the heart tissue found pronounced deficiency of LAMP2 protein in cardiomyocytes, alongside high expression in interstitial cells, which may explain the severity of cardiac involvement. Comparable cases support this observation, Bottilo et al. described a 23-year-old female with a novel *LAMP2* frameshift variant who developed early-onset hypertrophic cardiomyopathy and required heart transplantation (106). Chen et al. reported a mosaic *LAMP2* variant in an asymptomatic mother of an affected child, with 20% of leukocytes carrying the pathogenic *LAMP2* gene variant (60). These cases illustrate how mosaicism can influence phenotypic expression across tissues.

Clinical implications and limitations

This case supports the importance of comprehensive ophthalmic examination, including structural and functional analysis of the retina, for suspected and complex systemic disorders such as Danon disease. While this report highlights the diagnostic value of ophthalmological findings in rare systemic diseases, such as Danon disease, some limitations should be acknowledged: since this study was based on a single-case design, the generalisability of the findings is limited. However, as more data is obtained over time, those findings may be expanded and refined. The longitudinal data of our patient showed a stable retinal function after five years. Further longitudinal data of functional and structural alterations would be of importance, especially in mosaic *LAMP2* gene variant female carriers.

Understanding retinal function in acquired retinal disease through electrophysiology - Paper IV

A central retinal vein occlusion, a common retinal vascular disorder, often causes retinal ischemia, leading to significant impairment of retinal function and rapid VA decline. CRVO is clinically categorised into non-ischemic and ischemic subtypes, with the last one associated with a poorer prognosis when left to follow its natural course. ERG enables accurate differentiation between the subtypes by objectively assessing retinal function. Intravitreal therapies, primarily with anti-VEGF and/or dexamethasone, are standard treatments for macular oedema in CRVO and other retinal diseases such as wet AMD (79). However, these treatments typically require long-term, repeated usage to preserve vision. Only a handful of studies have examined the long-term impact of intravitreal therapies on photoreceptor cell function in CRVO eyes using ERG with varying results (71-73).

In paper IV, we conducted a retrospective study to investigate the long-term effects of intravitreal therapy on retinal structure and function in eyes with CRVO. Specifically, we assessed whether repeated intravitreal therapy, with anti-VEGF and/or dexamethasone, have an impact on photoreceptor cell function by comparing treated with untreated CRVO eyes.

Retinal function was evaluated using ffERG, in combination with VA and assessment of the macular structure using OCT. To the best of our knowledge, this is the first study to evaluate total retinal function using ffERG over a 4-year follow-up period in CRVO eyes receiving anti-VEGF and/or dexamethasone therapy, with a comparison to untreated CRVO eyes.

The effect of intravitreal treatment on visual acuity and foveal thickness

Our findings revealed a significant improvement in VA in the treated CRVO group, with a mean follow-up of approximately 6.5 years (final visit). The average visual gain was 10.7 ETDRS letters from baseline to the final visit. This is consistent with previous studies, including the well-recognised RETAIN study, which demonstrated similar VA improvements over a 4-year follow-up (70). Similarly, Spooner et al. reported a gain of approximately 9.5 letters at 5-year follow-up, and 14 ETDRS letters at 8 years, in CRVO eyes treated with anti-VEGF agents (107). However, other studies have reported more modest or even negative outcomes. For example, Chatziralli et al. reported a gain of approximately 6.9 ETDRS letters over a 4-year follow-up with anti-VEGF treatment (ranibizumab) (108), while Shah et al. reported a loss of 5 ETDRS letters in non-ischemic CRVO and a loss of 24 letters in ischemic CRVO after anti-VEGF treatment at 7-year follow-up (109). In contrast, our subgroup analysis, of the treated group revealed a gain of 12 ETDRS letters in non-ischemic CRVO eyes, and a gain of 9.6 letters in the ischemic group at final visit. This highlights the potential long-term benefit of sustained intravitreal treatments for macular oedema in CRVO eyes.

The mean CFT improved significantly, in both the treated (non-ischemic and ischemic) and non-treated CRVO groups and remained significantly reduced at final visit (6.5 years). This is consistent with several previous studies (69, 108). Notably, the mean CFT was found to be non-significantly thinner in the treated non-ischemic group, compared both to the ischemic and untreated CRVO groups, at final visit. Comparable results were reported by Spooner et al. in non-ischemic CRVO eyes at an 8-year follow-up (107). This is a rarely reported, and perhaps rarely observed, finding, making it difficult to determine whether the thinning is caused by anti-VEGF treatment, the disease itself, or a combination of both. Further analyses are needed, perhaps incorporating multifocal ERG, to better assess central retinal function in these patients.

The effect of intravitreal treatment on retinal function

While there are numerous studies focusing on VA and CFT outcomes in CRVO eyes treated with anti-VEGF, there is a notable gap in the literature concerning long-term retinal functional outcomes, particularly assessment by ERG and comparisons with untreated CRVO eyes. Most ERG studies on CRVO, evaluating anti-VEGF treatments, report only short-term outcomes, often with inconsistent results (71-73). In the present study, long-term ERG assessments revealed a significant reduction in both a- and b-wave amplitudes of the combined rod-cone response in both treated and untreated CRVO eyes after four years. Most treated eyes had received serial intravitreal injections with anti-VEGF primarily of aflibercept. This reduction

suggests a progressive decline in total retinal function, affecting both rod and cone photoreceptors, regardless of treatment status. Our findings are in line with those reported by Nishimura et al., who observed a similar decline in a- and b-wave amplitudes of combined rod-cone responses following one year of serial aflibercept injections (71). Additionally, Gardašević Topčić et al. reported reduced a-wave amplitudes in treated ischemic CRVO eyes following anti-VEGF therapy with bevacizumab for one year (73). These findings suggest that although intravitreal therapy is effective in controlling macular oedema and maintaining visual acuity, it does not seem to preserve the long-term photoreceptor function.

Further, the treated CRVO eyes, both ischemic and non-ischemic, exhibited a shortening of implicit times from baseline to follow-up (ERGII) in several ERG responses. These included the b-wave of the rod response, the a-wave of the combined rod-cone response, the single-flash response, and the b-wave of the 30 Hz flicker response. Similar findings were reported by Nishimura et al. (71), who observed shortened implicit times of 30 Hz flicker in treated, non-ischemic CRVO eyes. They hypothesised that intraretinal haemorrhage may act as an optical density filter, partially absorbing the light stimulus and thereby delaying the response of the photoreceptors. With resolution of haemorrhage, this filtering effect diminishes, leading to shortening of the implicit time (71). Yasuda et al. also reported shortened implicit times in the 30 Hz flicker response as early as one month after intravitreal ranibizumab injection (72). They offered two possible explanations, by drawing conclusions from the studies by Sophie et al. (110) and Campochiaro et al. (111) One conclusion being that anti-VEGF treatment reduces areas of retinal ischemia, thereby supporting functional recovery of the retina and shortening of implicit times, and the second, that elevated intraocular VEGF levels contribute to widespread macular and retinal oedema, which in turn impairs retinal signaling and prolongs implicit times. The resolution of oedema following anti-VEGF therapy may therefore restore more efficient signal transmission, reflected in shorter implicit times (72). In the present study, even though treated CRVO eyes demonstrated shortened implicit times, this was accompanied by reduced ERG amplitudes across nearly all light-stimulated responses in both treated and untreated groups. This widespread reduction in amplitudes reflects a sustained decline in the entire retina at the 4-year follow-up, suggesting long-term functional impact of CRVO itself on retinal function. Thus, the observed shortening of implicit times in treated CRVO eyes likely does not reflect a true improvement in retinal function. Instead, it may be attributed to enhanced signal transduction following the resolution of retinal oedema and haemorrhage as a secondary effect of anti-VEGF therapy.

Some limitations of the study should be acknowledged. One limitation is the variation in follow-up duration from baseline (ERGI) to follow-up (ERGII) between the treated and non-treated groups. However, this retrospective study was conducted in a real-world clinical setting between 2012 and 2022, a period that included the COVID-19 pandemic (2019-2023). We have considered that the longer time gap in

the non-treated group might have influenced outcomes by allowing for more natural ischemic progression. Nonetheless, when comparing non-treated vs treated groups' baseline clinical parameters, such as younger mean age (mean 66.5 vs. 69.8 years) and better baseline BCVA (mean 63.1 vs. 47.4), to follow-up BCVA values (mean 67.1 vs. 58.1), we tend to believe that the time gap did not significantly affect the progression of retinal ischemia or the comparative results between the groups. Furthermore, various anti-VEGF treatments were used (however, predominantly aflibercept). Concerning this, we suggest that these therapies have a similar impact on retinal function. Therefore, we believe that this difference in the specific drug used is unlikely to have influenced the overall findings of our study. Another important consideration is the limited number of eyes in the control (non-treated) CRVO group. At first glance, the treated and untreated groups may appear disparate, particularly since the untreated eyes did not exhibit macular oedema. However, our classification was based on the ischemic status of CRVO, distinguishing between non-ischemic and ischemic types. In the non-treated group, 6 out of 10 (60%) of eyes were classified as non-ischemic, while in the treated group 13 out of 28 (46%) eyes were non-ischemic. Despite the small sample size, these findings suggest that the two groups were not fundamentally dissimilar.

Conclusions

This thesis contributes to a deeper understanding of retinal structure, through the use of OCT, and functional changes, through the use of ERG, in inherited and acquired retinal diseases. This, in turn, contributes to more accurate diagnosis, facilitates monitoring and fosters a better understanding of disease progression and the potential development of targeted therapies.

Papers I, II Address the macular curvature as a novel and potentially valuable biomarker in RP, using an OCT-based method with enhanced accuracy and reproducibility. This method provides a reliable approach to assessing structural changes in the macular region and deepens our understanding of RP as a multifaceted retinal disease.

Paper III This report highlights the role of ophthalmological examination in diagnosing rare systemic diseases. The ophthalmologic findings can precede, accompany, or sometimes dominate the systemic disease, making retinal assessments crucial in early diagnosis. The described case further illustrated how mosaicism can shape phenotypic heterogeneity and the importance of assessing mosaicism across tissues, especially when counselling patients about prognosis and family planning. Moreover, the case described in our study emphasises the importance and need for interdisciplinary collaboration between departments. An accurate diagnosis and potential management of multiorgan disease, such as complex and severe Danon disease, would have been misdiagnosed or overlooked, without a coordinated effort from cardiology, ophthalmology, genetics and histopathology.

Paper IV Long-term visual outcomes improved in the treated group but remained unchanged in the non-treated group. While mean CFT improved in both groups, retinal function declined similarly over 4 years. This seems to suggest that the natural course of CRVO, rather than the treatment, is what primarily determines long-term retinal function. Additionally, it appears that anti-VEGF agents did not seem to impair photoreceptor cell function in either ischemic or non-ischemic CRVO eyes, though this also requires further investigation.

Challenges and future perspectives

Inherited retinal degenerative diseases exhibit extensive genotypic and phenotypic heterogenicity, posing significant challenges for the development of effective treatment strategies. Despite this complexity, the eye presents an ideal model suited for genetic research and therapeutic targets due to its accessibility, its immune-privilege status and the availability of non-invasive techniques for structural and functional assessment, such as OCT and ERG. In recent years, substantial progress has been made in the field of ophthalmic genetics. In 2017, the FDA approved the first gene therapy for an ophthalmic condition, voretigene neparvovec (LUXTURNA), which uses an adeno-associated viral (AAV) vector to deliver a functional copy of the *RPE65* gene through subretinal injection for the treatment of *RPE65*-associated LCA (112). This was a landmark event and a turning point in ophthalmology, as it spurred further research and the development of new therapeutic strategies for IRDs, offering renewed hope to patients worldwide (113). Another successful example of AAV-vector based gene therapy for inherited diseases was recently reported by Greenberg et al., in this phase I study in which seven male patients under the age of 21, with genetically confirmed Danon disease, received a single infusion of RP-A501, a recombinant AAV serotype 9 carrying the *LAMP2B* gene, which encodes an isoform of LAMP2 protein. Cardiac expression of LAMP2 protein was observed in six patients, along with improvement and/or stabilisation of the cardiac disease over a follow-up period of 24 to 54 months (114).

Gene therapy represents a significant advancement, supported by many years of clinical research. So far, gene therapy has demonstrated a high specificity, targeting specific gene variants. This limits its applicability to a broader group of patients due to the genetic heterogeneity of IRDs. New methods are emerging in the field of gene therapy. Techniques such as antisense oligonucleotide-based therapy, for instance targeting *CEP290*-RP, and CRISPR gene editing are under development (115). These approaches may potentially be applied in a wider population of IRD patients in the future. In parallel with gene therapy, other therapeutic strategies are being explored. Cell replacement therapy, with the potential to replace lost photoreceptors or RPE cells, may offer treatment options for a broader range of IRD patients (113) and perhaps patients with acquired retinal degenerative disease.

In contrast to gene therapy, anti-VEGF treatment is widely applied across a broad spectrum of retinal diseases and has demonstrated high efficacy in managing macular oedema, particularly in conditions such as CRVO, AMD and diabetic

retinopathy. Currently, anti-VEGF agents must be administered repeatedly over time in most of the patients with the above-mentioned retinal conditions. The findings presented in paper IV suggest that anti-VEGF therapy appears to be safe and does not seem to harm photoreceptor cells, even in the ischemic type of CRVO, despite repeated intravitreal injections. However, a major challenge remains to develop long-acting treatments that can be individualised and administered at the optimal time for each patient. Clinical evidence indicates that responses to anti-VEGF therapy vary considerably among patients with CRVO and other retinal diseases. In my opinion, this emphasises the need for the identification of structural, functional, or genetic biomarkers that can tailor a personalised regimen in terms of drug type, dosage, and injection interval. Moreover, there is a need for the development of long-term lasting agents, or perhaps smart drug delivery systems. For instance, in my opinion, implantable devices capable of detecting elevated intraocular VEGF levels and releasing the appropriate drug dose in real time, like the insulin pumps used in type 1 diabetes patients. This might represent a promising path for reducing the treatment burden, for the patients and the department, while maintaining therapeutic efficacy. Ultimately, the ideal scenario would be a one-time treatment that targets the underlying cause of the disease. In this regard, gene therapy holds significant potential, offering the possibility of a curative approach that could eliminate the need for the repeated intravitreal therapy.

As regards the understanding of the structural changes of the posterior pole, specifically in the macular region, the macular curvature could serve as a novel and potentially valuable biomarker in RP. Several studies have continued to investigate the macular region in RP, using similar OCT-based imaging techniques, as performed pivotally in papers I and II (116). Various theories have been proposed, yet no definitive explanation has been found for the observed alterations. It remains unclear whether increased macular curvature is protective or degenerative for retinal cells, or simply a secondary effect. In my opinion, future research may perhaps provide insight into the mechanisms of structural alteration and the implication on photoreceptor cell function. In my future research, following the completion of my dissertation, I aim to continue exploring this fascinating field of ophthalmology by studying retinal structure and function. One upcoming project will focus on assessing the macular curvature in patients with early onset retinal dystrophies, and particularly those with LCA and with XLRP gene variants, to investigate genotype and phenotype correlations in IRDs associated with macular staphylomas. A second project will examine both retinal functions, using ERG, and retinal structure, using OCT, in patients with adult-onset vitelliform macular dystrophy, with the goal of identifying correlations with underlying genetic findings.

Regardless of which therapeutic strategy ultimately proves to be most effective, continued research and innovation are essential in the search for treatments for inherited and acquired retinal degenerative diseases. Assessing structural and functional changes of the retina, especially in macular region, is important, as the

benefit of today's and probably future therapies lies in preserving still viable photoreceptors that also need proper structural conditions for their survival.

Acknowledgements

I would like to express my heartfelt thanks to all those who have supported me throughout my research and the writing of this thesis. Your encouragement, patience, and optimism have been invaluable to me, and I will forever remember your thoughtfulness.

I am deeply grateful to the following people:

Sten Andreasson, Professor and co-supervisor, thank you for introducing me into to the fascinating world of ERG and IRDs. Your ever-enchanting optimism and encouragement throughout the good and tough times. Your humbleness and open-door policy, your assurance that there are no stupid questions, and your ability to always find solutions even when it gets complicated.

Elisabeth Wittström, co-supervisor and colleague. You have been an inspiration in every sense: in research, clinical practice, and in life. Your sharp intellect and diagnostic precision are truly remarkable, often reaching the correct conclusion in the blink of an eye. No challenge is ever too great; you pursue answers with unwavering determination, even if it means reanalysing an entire genome, and as always, you are right. It has been a privilege to learn from and work alongside you during these research years. I look forward to continuing our collaboration in the future.

Maria Thereza Perez, main supervisor, associated professor. Thank you for stepping in as my main supervisor and for your unwavering support and guidance throughout this research journey. Your experience and sharp research insight have been invaluable in shaping me into the independent researcher I am becoming. Yet I know I still have a lot to learn and that this journey will not end with this thesis!

Ulrika Kjellström, co-supervisor, associated professor, colleague. Thank you for your immense support and countless hours of proofreading throughout this PhD thesis. Your remarkable eye for detail and ability to shape text into clear, meaningful sentences without losing its essence is truly admirable. You've kept me on track whenever I got lost, always ensuring that everything was completed on time and to the highest standard.

Hiroki Tersaki, Professor, co-supervisor in Japan, thank you for welcoming me into your research team at Nagoya Medical University. Your infectious optimism and energy are truly inspiring. I'll always remember the many-hours-long

experimental macular hole transplant surgery, an unforgettable experience, and the many delicious Japanese meals and interesting discussions we shared along the way.

Shinji Ueno, co-supervisor in Japan. You introduced me to the fascinating world of ERG at Nagoya University and innovative research methods, while also sharing the richness of Japanese culture. Thank you for taking me under your wing during a challenging time - as I was just beginning my PhD journey and learning to navigate life in Japan.

Shiori, Akira, Taro, thank you to my fellow research colleagues at Nagoya University for your support during the Japanese projects. You made me feel welcome and helped me navigate, not only the datasets and Japanese computer systems, but also life in Nagoya.

Mika, at the Dean's office at the Nagoya University, Graduate School of Medicine. Without your support and help, to navigation through Japanese paperwork, I don't think I would have made it to Nagoya. Thank you for your time and patience.

Magdalena Naumovska, colleague, from countless 'fika pauser' filled with conversations about everything between heaven and earth, to tackling impossible tasks with creativity and laughter - you bring energy, insight, and cleverness to every moment. Your bubbly spirit, sharp clinical instincts, and ability to find clever solutions make you one of a kind. Working with you is like sharing a glass of champagne: uplifting, sparkling, and joyful.

Tove Faxen, colleague, my wingwomen, from the first days at the ophthalmology department. A superwoman both at the clinic and at home, who sometimes feels like my big sister. You inspire me with your thoughtful questions and honesty and down-to-earth approach.

Andreas Nilsson, colleague, my wingman, you approach the most things in work and life with humbleness, calmness and cleverness. Also, my roommate and probably has the cleanest desk in the Department of Ophthalmology.

Kajsa Tenland, colleague, your calm and gentle presence brings a sense of peace. You are always ready with a warm smile and an open heart. Your cleverness, paired with your humbleness, is truly remarkable and deeply appreciated.

Hanna-Maria Öhnell and **Lotta Gränse**, collogues, like Chip and Dale, always together, not in a mischievous way, but in a clever, humble, and truly awesome way. You're a rock in research and at the clinic, consistently brilliant, and always keeping the best interests of even the smallest patients at heart. It's a joy and privilege to work alongside you.

All the wonderful colleagues in the Ophthalmology Department at Skåne University Hospital who make every day at work so much more interesting, rewarding and fun! Elin Gunnlaugsdottir, Johanna Berggren, Ellen Sönnergren, Pegah Torabi, Jenny Hult, Cu Dybelius Ansson, Stellan Molander, Johanna Sundgren, Sigridur

My heartfelt thanks go to the anonymous hand whose illustration work added both clarity and color to this thesis. After all, a picture is worth a thousand words.

Julian Meinert, ジュリアン，the Meinert family´s artist, always in tune with Japanese and global trends from Berlin, thoughtfully designed the front page of this thesis with creativity and precision.

Aljona Rukavishnikova, friend, whose support and encouragement kept me motivated, even through the challenging moments of this PhD journey.

Marianna Boscariol, friend, to my Brazilian soul-twin in Japan - life became so much more vibrant and meaningful thanks to you. You shared with me the richness of Japanese history and culture, lifted my spirits when I needed it most, and showed me how to stay strong in both body and mind. I'm forever grateful for your presence on this journey.

Karin, Linnea, Cecilia and **Sandra** - my childhood squad, still going strong after all these years! There's nothing I can't share with you, no complaint too small, and no hour too late. You've always had my back, and for that, I'm endlessly grateful.

Matthias, my love, my best friend and husband - life is so much more colourful with you. Your honesty is unmatched. You teach me to appreciate life and find joy in the little things. No one can make me smile the way you do, even in the darkest moments. With you by my side, nothing seems impossible.

Emma, to my beloved daughter - the apple of my eye. Your presence lights up every room, your curious questions and thoughtful observations reveal the little researcher in you, and the joy you bring into our life is beyond words.

Mum and **Dad,** thank you for your unwavering support throughout this journey (and life) and for always believing in me. You know how to lift my spirits. Mum, you taught me to fight and never give up, even when life seems impossible. Dad, you showed me that hard work, dedication and resilience are always rewarded. I love you.

Thank you! アリガトウ!

References

1. Arshavsky VY, Lamb TD, Pugh EN, Jr. G proteins and phototransduction. Annu Rev Physiol. 2002;64:153-87.

2. Hille B. Electrical signals and ion movement. In: Kandel ER, Schwartz JH, Jessell TM, Siegelbaum SA, Hudspeth AJ, editors. Principles of Neural Science, 5th Ed. New York: McGraw-Hill Education; 2014. p. 165-240.

3. Holmgren F. method att objectivera effekten av ljusintryck på retina. Upsala Läkareförenings Förhandlingar. 1865; 1:184-98.

4. Dewar J. The physiological action of light. Nature. 1877;15:433-5.

5. Carr RE, Siegel IM. Action spectrum of the human early receptor potential. Nature. 1970;225(5227):88-9.

6. Penn RD, Hagins WA. Signal transmission along retinal rods and the origin of the electroretinographic a-wave. Nature. 1969;223(5202):201-4.

7. Green DG, Kapousta-Bruneau NV. A dissection of the electroretinogram from the isolated rat retina with microelectrodes and drugs. Vis Neurosci. 1999;16(4):727-41.

8. Tian N, Slaughter MM. Correlation of dynamic responses in the ON bipolar neuron and the b-wave of the electroretinogram. Vision Res. 1995;35(10):1359-64.

9. Miller RF, Dowling JE. Intracellular responses of the Müller (glial) cells of mudpuppy retina: their relation to b-wave of the electroretinogram. J Neurophysiol. 1970;33(3):323-41.

10. Nilsson SE, Skoog KO. Covariation of the simultaneously recorded c-wave and standing potential of the human eye. Acta Ophthalmol (Copenh). 1975;53(5):721-30.

11. Kolb H. Fernandez E, Jonas B. et al. The Electroretinogram and Electro-oculogram: Clinical Applications. 2005. In: Webvision: The Organization of the Retina and Visual System [Internet]. Salt Lake City (UT): University of Utah Health Sciences Center. Available from: https://www.ncbi.nlm.nih.gov/books/NBK11553/.

12. Marmor MF, Arden, G. B., Nilsson, S.-E., & Zrenner, E. Standard for clinical electroretinography. Documenta Ophthalmologica. 1989;107: 816–9.

13. Robson AG, Frishman LJ, Grigg J, Hamilton R, Jeffrey BG, Kondo M, et al. ISCEV Standard for full-field clinical electroretinography (2022 update). Doc Ophthalmol. 2022;144(3):165-77.

14. Sutter EE, Tran D. The field topography of ERG components in man-I. The photopic luminance response. Vision Res. 1992;32(3):433-46.

15. Hoffmann MB, Bach M, Kondo M, Li S, Walker S, Holopigian K, et al. ISCEV standard for clinical multifocal electroretinography (mfERG) (2021 update). Doc Ophthalmol. 2021;142(1):5-16.

16. London A, Benhar I, Schwartz M. The retina as a window to the brain - from eye research to CNS disorders. Nature Reviews Neurology. 2013;9(1):44-53.

17. Curcio CA, Sloan KR, Kalina RE, Hendrickson AE. Human photoreceptor topography. J Comp Neurol. 1990;292(4):497-523.

18. Bowmaker JK, Dartnall HJ. Visual pigments of rods and cones in a human retina. J Physiol. 1980;298:501-11.

19. Osterberg G. Topography of the layer of rods and cones in the human retina. Acta Ophthal Suppl. 1935;6:1–103.

20. Curcio CA, Sloan KR, Jr., Packer O, Hendrickson AE, Kalina RE. Distribution of cones in human and monkey retina: individual variability and radial asymmetry. Science. 1987;236(4801):579-82.

21. Mahabadi N, Al Khalili Y. Neuroanatomy, Retina Treasure Island (FL): StatPearls Publishing; 2023 [Available from: https://www.ncbi.nlm.nih.gov/books/NBK545310/.

22. Kolb H, Fernandez E, Jones B. The Organization of the Retina and Visual System in Webvision [Internet]. https://webvision.med.utah.edu/book/electrophysiology/the-electroretinogram-erg/: Salt Lake City (UT): University of Utah Health Sciences Center; 1995- 2005

23. Bone RA, Landrum JT, Tarsis SL. Preliminary identification of the human macular pigment. Vision Res. 1985;25(11):1531-5.

24. Polyak. The Retina: The Anatomy and the Histology of the Retina in Man, Ape, and Monkey, Including the Consideration of Visual Functions, the History of Physiological Optics, and the Histological Laboratory Technique. New England Journal of Medicine 1942;227 (6):239.

25. Yamada E. Some structural features of the fovea centralis in the human retina. Arch Ophthalmol. 1969;82(2):151-9.

26. Jonas JB, Schneider U, Naumann GO. Count and density of human retinal photoreceptors. Graefes Arch Clin Exp Ophthalmol. 1992;230(6):505-10.

27. Kolb H, Fernandez, E, Nelson R. The organization of the retina and visual system in Webvision [Internet] Salt Lake City (UT): University of Utah Health Sciences Center; 2010 Available from: https://webvision.med.utah.edu/book/part-i-foundations/simple-anatomy-of-the-retina/.

28. Masland RH. The neuronal organization of the retina. Neuron. 2012;76(2):266-80.

29. de Melo Reis RA, Ventura AL, Schitine CS, de Mello MC, de Mello FG. Müller glia as an active compartment modulating nervous activity in the vertebrate retina: neurotransmitters and trophic factors. Neurochem Res. 2008;33(8):1466-74.

30. Lakkaraju A, Umapathy A, Tan LX, Daniele L, Philp NJ, Boesze-Battaglia K, et al. The cell biology of the retinal pigment epithelium. Prog Retin Eye Res. 2020:100846.

31. Strauss O. The retinal pigment epithelium in visual function. Physiol Rev. 2005;85(3):845-81.

32. Kiel JW. Anatomy. In: Kiel JW. The Ocular Circulation. San Rafael (CA): Morgan & Claypool Life Sciences; 2010. Available from https://www.ncbi.nlm.nih.gov/books/NBK53329/.

33. Fujimoto J, Swanson E. The Development, Commercialization, and Impact of Optical Coherence Tomography. Invest Ophthalmol Vis Sci. 2016;57(9):Oct1-oct13.

34. Spaide RF, Curcio CA. Anatomical correlates to the bands seen in the outer retina by optical coherence tomography: literature review and model. Retina. 2011;31(8):1609-19.

35. Sousa K, Fernandes T, Gentil R, Mendonça L, Falcão M. Outer retinal layers as predictors of visual acuity in retinitis pigmentosa: a cross-sectional study. Graefes Arch Clin Exp Ophthalmol. 2019;257(2):265-71.

36. Kominami T, Ueno S, Kominami A, Nakanishi A, Yasuda S, Piao CH, et al. Associations Between Outer Retinal Structures and Focal Macular Electroretinograms in Patients With Retinitis Pigmentosa. Invest Ophthalmol Vis Sci. 2017;58(12):5122-8.

37. Birch DG, Locke KG, Wen Y, Locke KI, Hoffman DR, Hood DC. Spectral-domain optical coherence tomography measures of outer segment layer progression in patients with X-linked retinitis pigmentosa. JAMA Ophthalmol. 2013;131(9):1143-50.

38. Hariri AH, Zhang HY, Ho A, Francis P, Weleber RG, Birch DG, et al. Quantification of Ellipsoid Zone Changes in Retinitis Pigmentosa Using en Face Spectral Domain-Optical Coherence Tomography. JAMA Ophthalmol. 2016;134(6):628-35.

39. Henderson RH. Inherited retinal dystrophies. Paediatrics and Child Health. 2020;30(1):19-27.

40. Bunker CH, Berson EL, Bromley WC, Hayes RP, Roderick TH. Prevalence of retinitis pigmentosa in Maine. Am J Ophthalmol. 1984;97(3):357-65.

41. Grøndahl J. Estimation of prognosis and prevalence of retinitis pigmentosa and Usher syndrome in Norway. Clin Genet. 1987;31(4):255-64.

42. Mansergh FC, Millington-Ward S, Kennan A, Kiang AS, Humphries M, Farrar GJ, et al. Retinitis pigmentosa and progressive sensorineural hearing loss caused by a C12258A mutation in the mitochondrial MTTS2 gene. Am J Hum Genet. 1999;64(4):971-85.

43. Kajiwara K, Berson EL, Dryja TP. Digenic retinitis pigmentosa due to mutations at the unlinked peripherin/RDS and ROM1 loci. Science. 1994;264(5165):1604-8.

44. Hartong DT, Berson EL, Dryja TP. Retinitis pigmentosa. Lancet. 2006;368(9549):1795-809.

45. Koenekoop RK, Wang H, Majewski J, Wang X, Lopez I, Ren H, et al. Mutations in NMNAT1 cause Leber congenital amaurosis and identify a new disease pathway for retinal degeneration. Nat Genet. 2012;44(9):1035-9.

46. Pierrache LHM, Kimchi A, Ratnapriya R, Roberts L, Astuti GDN, Obolensky A, et al. Whole-Exome Sequencing Identifies Biallelic IDH3A Variants as a Cause of Retinitis Pigmentosa Accompanied by Pseudocoloboma. Ophthalmology. 2017;124(7):992-1003.

47. Ajmal M, Khan MI, Neveling K, Khan YM, Azam M, Waheed NK, et al. A missense mutation in the splicing factor gene DHX38 is associated with early-onset retinitis pigmentosa with macular coloboma. J Med Genet. 2014;51(7):444-8.

48. Yzer S, Hollander AI, Lopez I, Pott JW, de Faber JT, Cremers FP, et al. Ocular and extra-ocular features of patients with Leber congenital amaurosis and mutations in CEP290. Mol Vis. 2012;18:412-25.

49. Ilhan A, Yolcu U, Diner O, Uzun S, Gundogan FC. Coexistence of Posterior Staphyloma, Retinitis Pigmentosa and Moderate Myopia. J Coll Physicians Surg Pak. 2016;26(1):70-1.

50. Xu X, Fang Y, Yokoi T, Shinohara K, Hirakata A, Iwata T, et al. POSTERIOR STAPHYLOMAS IN EYES WITH RETINITIS PIGMENTOSA WITHOUT HIGH MYOPIA. Retina. 2019;39(7):1299-304.

51. Ohno-Matsui K. Proposed Classification of Posterior Staphylomas Based on Analyses of Eye Shape by Three-Dimensional Magnetic Resonance Imaging and Wide-Field Fundus Imaging. Ophthalmology. 2014;121(9):1798-809.

52. Danon MJ, Oh SJ, DiMauro S, Manaligod JR, Eastwood A, Naidu S, et al. Lysosomal glycogen storage disease with normal acid maltase. Neurology. 1981;31(1):51-7.

53. Prall FR, Drack A, Taylor M, Ku L, Olson JL, Gregory D, et al. Ophthalmic manifestations of Danon disease. Ophthalmology. 2006;113(6):1010-3.

54. Schorderet DF, Cottet S, Lobrinus JA, Borruat FX, Balmer A, Munier FL. Retinopathy in Danon disease. Arch Ophthalmol. 2007;125(2):231-6.

55. Nishino I, Fu J, Tanji K, Yamada T, Shimojo S, Koori T, et al. Primary LAMP-2 deficiency causes X-linked vacuolar cardiomyopathy and myopathy (Danon disease). Nature. 2000;406(6798):906-10.

56. Boucek D, Jirikowic J, Taylor M. Natural history of Danon disease. Genet Med. 2011;13(6):563-8.

57. Thiadens AA, Slingerland NW, Florijn RJ, Visser GH, Riemslag FC, Klaver CC. Cone-rod dystrophy can be a manifestation of Danon disease. Graefes Arch Clin Exp Ophthalmol. 2012;250(5):769-74.

58. Sugie K, Yamamoto A, Murayama K, Oh SJ, Takahashi M, Mora M, et al. Clinicopathological features of genetically confirmed Danon disease. Neurology. 2002;58(12):1773-8.

59. Takahashi M, Yamamoto A, Takano K, Sudo A, Wada T, Goto Y, et al. Germline mosaicism of a novel mutation in lysosome-associated membrane protein-2 deficiency (Danon disease). Ann Neurol. 2002;52(1):122-5.

60. Chen XL, Zhao Y, Ke HP, Liu WT, Du ZF, Zhang XN. Detection of somatic and germline mosaicism for the LAMP2 gene mutation c.808dupG in a Chinese family with Danon disease. Gene. 2012;507(2):174-6.

61. Cugati S, Wang JJ, Knudtson MD, Rochtchina E, Klein R, Klein BE, et al. Retinal vein occlusion and vascular mortality: pooled data analysis of 2 population-based cohorts. Ophthalmology. 2007;114(3):520-4.

62. Stem MS, Talwar N, Comer GM, Stein JD. A longitudinal analysis of risk factors associated with central retinal vein occlusion. Ophthalmology. 2013;120(2):362-70.

63. Kolar P. Risk factors for central and branch retinal vein occlusion: a meta-analysis of published clinical data. J Ophthalmol. 2014;2014:724780.

64. Hayreh SS, Podhajsky PA, Zimmerman MB. Natural history of visual outcome in central retinal vein occlusion. Ophthalmology. 2011;118(1):119-33.e1-2.

65. Pe'er J, Folberg R, Itin A, Gnessin H, Hemo I, Keshet E. Vascular endothelial growth factor upregulation in human central retinal vein occlusion. Ophthalmology. 1998;105(3):412-6.

66. Aiello LP, Avery RL, Arrigg PG, Keyt BA, Jampel HD, Shah ST, et al. Vascular endothelial growth factor in ocular fluid of patients with diabetic retinopathy and other retinal disorders. N Engl J Med. 1994;331(22):1480-7.

67. Varma R, Bressler NM, Suñer I, Lee P, Dolan CM, Ward J, et al. Improved vision-related function after ranibizumab for macular edema after retinal vein occlusion: results from the BRAVO and CRUISE trials. Ophthalmology. 2012;119(10):2108-18.

68. Ogura Y, Roider J, Korobelnik JF, Holz FG, Simader C, Schmidt-Erfurth U, et al. Intravitreal aflibercept for macular edema secondary to central retinal vein occlusion: 18-month results of the phase 3 GALILEO study. Am J Ophthalmol. 2014;158(5):1032-8.

69. Heier JS, Clark WL, Boyer DS, Brown DM, Vitti R, Berliner AJ, et al. Intravitreal aflibercept injection for macular edema due to central retinal vein occlusion: two-year results from the COPERNICUS study. Ophthalmology. 2014;121(7):1414-20.e1.

70. Campochiaro PA, Sophie R, Pearlman J, Brown DM, Boyer DS, Heier JS, et al. Long-term outcomes in patients with retinal vein occlusion treated with ranibizumab: the RETAIN study. Ophthalmology. 2014;121(1):209-19.

71. Nishimura T, Machida S, Hara Y. Changes of focal macular and full-field electroretinograms after intravitreal aflibercept in patients with central retinal vein occlusion. Doc Ophthalmol. 2020;141(2):169-79.

72. Yasuda S, Kachi S, Ueno S, Piao CH, Terasaki H. Flicker electroretinograms before and after intravitreal ranibizumab injection in eyes with central retinal vein occlusion. Acta Ophthalmol. 2015;93(6):e465-8.

73. Gardašević Topčić I, Šuštar M, Brecelj J, Hawlina M, Jaki Mekjavić P. Morphological and electrophysiological outcome in prospective intravitreal bevacizumab treatment of macular edema secondary to central retinal vein occlusion. Doc Ophthalmol. 2014;129(1):27-38.

74. Larsson J, Bauer B, Andréasson S. The 30-Hz flicker cone ERG for monitoring the early course of central retinal vein occlusion. Acta Ophthalmol Scand. 2000;78(2):187-90.

75. Johnson MA, Marcus S, Elman MJ, McPhee TJ. Neovascularization in central retinal vein occlusion: electroretinographic findings. Arch Ophthalmol. 1988;106(3):348-52.

76. Hayreh SS, Klugman MR, Beri M, Kimura AE, Podhajsky P. Differentiation of ischemic from non-ischemic central retinal vein occlusion during the early acute phase. Graefes Arch Clin Exp Ophthalmol. 1990;228(3):201-17.

77. Shweiki D, Itin A, Soffer D, Keshet E. Vascular endothelial growth factor induced by hypoxia may mediate hypoxia-initiated angiogenesis. Nature. 1992;359(6398):843-5.

78. Kliffen M, Sharma HS, Mooy CM, Kerkvliet S, de Jong PT. Increased expression of angiogenic growth factors in age-related maculopathy. Br J Ophthalmol. 1997;81(2):154-62.

79. Rosenfeld PJ, Brown DM, Heier JS, Boyer DS, Kaiser PK, Chung CY, et al. Ranibizumab for neovascular age-related macular degeneration. N Engl J Med. 2006;355(14):1419-31.

80. Korobelnik JF, Kodjikian L, Delcourt C, Gualino V, Leaback R, Pinchinat S, et al. Two-year, prospective, multicenter study of the use of dexamethasone intravitreal implant for treatment of macular edema secondary to retinal vein occlusion in the clinical setting in France. Graefes Arch Clin Exp Ophthalmol. 2016;254(12):2307-18.

81. Dryja TP, McGee TL, Reichel E, Hahn LB, Cowley GS, Yandell DW, et al. A point mutation of the rhodopsin gene in one form of retinitis pigmentosa. Nature. 1990;343(6256):364-6.

82. Dryja TP, McGee TL, Hahn LB, Cowley GS, Olsson JE, Reichel E, et al. Mutations within the rhodopsin gene in patients with autosomal dominant retinitis pigmentosa. N Engl J Med. 1990;323(19):1302-7.

83. Moussa G, Bassilious K, Mathews N. A novel excel sheet conversion tool from Snellen fraction to LogMAR including 'counting fingers', 'hand movement', 'light perception' and 'no light perception' and focused review of literature of low visual acuity reference values. Acta Ophthalmol. 2021;99(6):e963-e5.

84. McCulloch DL, Kondo M, Hamilton R, Lachapelle P, Messias AMV, Robson AG, et al. ISCEV extended protocol for the stimulus–response series for light-adapted full-field ERG. Documenta Ophthalmologica. 2019;138(3):205-15.

85. Johnson MA, Jeffrey BG, Messias AMV, Robson AG. ISCEV extended protocol for the stimulus-response series for the dark-adapted full-field ERG b-wave. Doc Ophthalmol. 2019;138(3):217-27.

86. Constable PA, Bach M, Frishman LJ, Jeffrey BG, Robson AG. ISCEV Standard for clinical electro-oculography (2017 update). Doc Ophthalmol. 2017;134(1):1-9.

87. Laíns I, Wang JC, Cui Y, Katz R, Vingopoulos F, Staurenghi G, et al. Retinal applications of swept source optical coherence tomography (OCT) and optical coherence tomography angiography (OCTA). Prog Retin Eye Res. 2021;84:100951.

88. Miyake M, Yamashiro K, Akagi-Kurashige Y, Oishi A, Tsujikawa A, Hangai M, et al. Analysis of fundus shape in highly myopic eyes by using curvature maps constructed from optical coherence tomography. PLoS One. 2014;9(9):e107923.

89. Delori FC, Dorey CK, Staurenghi G, Arend O, Goger DG, Weiter JJ. In vivo fluorescence of the ocular fundus exhibits retinal pigment epithelium lipofuscin characteristics. Invest Ophthalmol Vis Sci. 1995;36(3):718-29.

90. Yung M, Klufas MA, Sarraf D. Clinical applications of fundus autofluorescence in retinal disease. Int J Retina Vitreous. 2016;2:12.

91. Marmor MF, Ravin JG. Fluorescein angiography: insight and serendipity a half century ago. Arch Ophthalmol. 2011;129(7):943-8.

92. Kanski Jack J. BB. Clinical Ophthalmology : A Systemic Approach. 7th ed. Edinburgh Elsevier; 2011.

93. Heijl AL, G.; Olsson, J. A package for the statistical analysis of visual fields In: Greve ELH, A. , editor. *Seventh International Visual Field Symposium*, Amsterdam, September 1986. Documenta Ophthalmological Proceedings Series 49. Dordrecht: Springer; 1987.

94. Numa S, Yamashiro K, Wakazono T, Yoshikawa M, Miyake M, Nakanishi H, et al. Prevalence of posterior staphyloma and factors associated with its shape in the Japanese population. Sci Rep. 2018;8(1):4594.

95. Takahashi A, Ito Y, Iguchi Y, Yasuma TR, Ishikawa K, Terasaki H. Axial length increases and related changes in highly myopic normal eyes with myopic complications in fellow eyes. Retina. 2012;32(1):127-33.

96. Hajali M, Fishman GA. The prevalence of cystoid macular oedema on optical coherence tomography in retinitis pigmentosa patients without cystic changes on fundus examination. Eye (Lond). 2009;23(4):915-9.

97. Arrigo A, Aragona E, Perra C, Bianco L, Antropoli A, Saladino A, et al. Characterizing macular edema in retinitis pigmentosa through a combined structural and microvascular optical coherence tomography investigation. Sci Rep. 2023;13(1):800.

98. Yoon CK, Bae K, Yu HG. Longitudinal Microstructure Changes of the Retina and Choroid in Retinitis Pigmentosa. Am J Ophthalmol. 2022;241:149-59.

99. Dhoot DS, Huo S, Yuan A, Xu D, Srivistava S, Ehlers JP, et al. Evaluation of choroidal thickness in retinitis pigmentosa using enhanced depth imaging optical coherence tomography. Br J Ophthalmol. 2013;97(1):66-9.

100. Morgan IG, Ohno-Matsui K, Saw SM. Myopia. Lancet. 2012;379(9827):1739-48.

101. Carr JC, Stone WS. The science behind myopia. In: Jones BW, Marc RE, editors. Webvision: The organization of the retina and visual system [Internet]. Salt Lake City (UT): University of Utah Health Sciences Center; 2010. Available from: https://webvision.med.utah.edu/

102. Tran M, Kolesnikova M, Kim AH, Kowal T, Ning K, Mahajan VB, et al. Clinical characteristics of high myopia in female carriers of pathogenic RPGR mutations: a case series and review of the literature. Ophthalmic Genet. 2023;44(3):295-303.

103. Koyanagi Y, Ueno S, Ito Y, Kominami T, Komori S, Akiyama M, et al. Relationship Between Macular Curvature and Common Causative Genes of Retinitis Pigmentosa in Japanese Patients. Invest Ophthalmol Vis Sci. 2020;61(10):6.

104. Hedberg Oldfors C, Máthé G, Thomson K, Tulinius M, Karason K, Östman-Smith I, et al. Early onset cardiomyopathy in females with Danon disease. Neuromuscul Disord. 2015;25(6):493-501.

105. Regelsberger G, Höftberger R, Pickl WF, Zlabinger GJ, Körmöczi U, Salzer-Muhar U, et al. Danon disease: case report and detection of new mutation. J Inherit Metab Dis. 2009;32 Suppl 1:S115-22.

106. Bottillo I, Giordano C, Cerbelli B, D'Angelantonio D, Lipari M, Polidori T, et al. A novel LAMP2 mutation associated with severe cardiac hypertrophy and microvascular remodeling in a female with Danon disease: a case report and literature review. Cardiovasc Pathol. 2016;25(5):423-31.

107. Spooner KL, Fraser-Bell S, Hong T, Wong JG, Chang AA. Long-term outcomes of anti-VEGF treatment of retinal vein occlusion. Eye (Lond). 2022;36(6):1194-201.

108. Chatziralli I, Theodossiadis G, Chatzirallis A, Parikakis E, Mitropoulos P, Theodossiadis P. RANIBIZUMAB FOR RETINAL VEIN OCCLUSION: Predictive Factors and Long-Term Outcomes in Real-Life Data. Retina. 2018;38(3):559-68.

109. Shah PN, Shanmugam MP, Vora UB, Agrawal S, Sirivella I, Suryakanth S, et al. Long-term real-world outcomes in retinal vein occlusions: How close are we to the trials? Indian J Ophthalmol. 2022;70(12):4370-5.

110. Sophie R, Hafiz G, Scott AW, Zimmer-Galler I, Nguyen QD, Ying H, et al. Long-term outcomes in ranibizumab-treated patients with retinal vein occlusion; the role of progression of retinal nonperfusion. Am J Ophthalmol. 2013;156(4):693-705.

111. Campochiaro PA, Bhisitkul RB, Shapiro H, Rubio RG. Vascular endothelial growth factor promotes progressive retinal nonperfusion in patients with retinal vein occlusion. Ophthalmology. 2013;120(4):795-802.

112. Russell S, Bennett J, Wellman JA, Chung DC, Yu ZF, Tillman A, et al. Efficacy and safety of voretigene neparvovec (AAV2-hRPE65v2) in patients with RPE65-mediated inherited retinal dystrophy: a randomised, controlled, open-label, phase 3 trial. Lancet. 2017;390(10097):849-60.

113. Chen HY, Lehmann OJ, Swaroop A. Genetics and therapy for pediatric eye diseases. EBioMedicine. 2021;67:103360.

114. Greenberg B, Taylor M, Adler E, Colan S, Ricks D, Yarabe P, et al. Phase 1 Study of AAV9.LAMP2B Gene Therapy in Danon Disease. N Engl J Med. 2025;392(10):972-83.

115. Pierce EA, Aleman TS, Jayasundera KT, Ashimatey BS, Kim K, Rashid A, et al. Gene Editing for CEP290-Associated Retinal Degeneration. N Engl J Med. 2024;390(21):1972-84.

116. Müller PL, Kihara Y, Olvera-Barrios A, Warwick AN, Egan C, Williams KM, et al. Quantification and Predictors of OCT-Based Macular Curvature and Dome-Shaped Configuration: Results From the UK Biobank. Invest Ophthalmol Vis Sci. 2022;63(9):28.